
Electronic Theses and Dissertations, 2004-2019

2004

Surface Chemistry Of Application Specific Pads And Copper Chemical Mechanical Planarization

Sameer Arun Deshpande
University of Central Florida



Part of the [Engineering Commons](#)

Find similar works at: <https://stars.library.ucf.edu/etd>

University of Central Florida Libraries <http://library.ucf.edu>

This Masters Thesis (Open Access) is brought to you for free and open access by STARS. It has been accepted for inclusion in Electronic Theses and Dissertations, 2004-2019 by an authorized administrator of STARS. For more information, please contact STARS@ucf.edu.

STARS Citation

Deshpande, Sameer Arun, "Surface Chemistry Of Application Specific Pads And Copper Chemical Mechanical Planarization" (2004). *Electronic Theses and Dissertations, 2004-2019*. 22.

<https://stars.library.ucf.edu/etd/22>

SURFACE CHEMISTRY OF APPLICATION SPECIFIC PADS AND COPPER
CHEMICAL MECHANICAL PLANARIZATION

by

SAMEER DESHPANDE
B.E. University of Pane, 2001

A thesis submitted in partial fulfillment of the requirements
for the degree of Master of Science
in the Department of Mechanical, Materials and Aerospace Engineering
in the College of Engineering and Computer Science
at the University of Central Florida
Orlando, Florida

Summer Term
2004

©2004 Sameer Deshpande

ABSTRACT

Advances in the interconnection technology have played a key role in the continued improvement of the integrated circuit (IC) density, performance and cost. Copper (Cu) metallization, dual damascenes processing and integration of copper with low dielectric constant material are key issues in the IC industries. Chemical mechanical planarization of copper (Cu-CMP) has emerged as an important process for the manufacturing of ICs. Usually, Cu-CMP process consists of several steps such as the removal of surface layer by mechanical action of the pad and the abrasive particles, the dissolution of the abraded particles in the CMP solution, and the protection of the recess areas. The CMP process occurs at the atomic level at the pad/slurry/wafer interface, and hence, slurries and polishing pads play critical role in its successful implementation.

The slurry for the Cu-CMP contains chemical components to facilitate the oxidation and removal of excess Cu as well as passivation of the polished surface. During the process, these slurry chemicals also react with the pad. In the present study, investigations were carried out to understand the effect of hydrogen peroxide (H_2O_2) as an oxidant and benzotriazole (BTA) as an inhibitor on the CMP of Cu. Interaction of these slurry components on copper has been investigated using electrochemical studies, x-ray photoelectron spectroscopy (XPS) and secondary ion mass spectroscopy (SIMS).

In the presence of 0.1M glycine, Cu removal rate was found to be high in the solution containing 5% H_2O_2 at pH 2 because of the Cu-glycine complexation reaction. The dissolution

rate of the Cu was found to increase due to the formation of highly soluble Cu-glycine complex in the presence of H₂O₂. Addition of 0.01M BTA in the solution containing 0.1M glycine and 5% H₂O₂ at pH 2 exhibited a reduction in the Cu removal rate due to the formation of Cu-BTA complex on the surface of the Cu further inhibiting the dissolution. XPS and SIMS investigations revealed the formation of such Cu-glycine complex, which help understand the mechanism of the Cu-oxidant-inhibitor interaction during polishing.

Along with the slurry, pads used in the Cu-CMP process have direct influence an overall process. To overcome problems associated with the current pads, new application specific pad (ASP) have been developed in collaboration with PsiloQuest Inc. Using plasma enhanced chemical vapor deposition (PECVD) process; surface of such ASP pads were modified. Plasma treatment of a polymer surface results in the formation of various functional groups and radicals. Post plasma treatment such as chemical reduction or oxidation imparts a more uniform distribution of such functional groups on the surface of the polymer resulting in unique surface properties.

The mechanical properties of such coated pad have been investigated using nano-indentation technique in collaboration with Dr. Vaidyanathan's research group. The surface morphology and the chemistry of the ASP are studied using scanning electron microscopy (SEM), x-ray photoelectron spectroscopy (XPS), and fourier transform infrared spectroscopy (FTIR) to understand the formation of different chemical species on the surface. It is observed that the mechanical and the chemical properties of the pad top surface are a function of the PECVD coating time. Such PECVD treated pads are found to be hydrophilic and do not require being stored in aqueous medium during the not-in-use period. The metal removal rate using such surface modified polishing pad is found to increase linearly with the PECVD coating time.

Overall, this thesis is an attempt to optimize the two most important parameters of the Cu-CMP process viz. slurry and pads for enhanced performance and ultimately reduce the cost of ownership (CoO).

ACKNOWLEDGEMENTS

I take this opportunity to thank Dr. Sudipta Seal (Faculty Advisor) for his support, motivation and valuable discussions during this entire research work. His constant encouragement for independent thinking and confidence in my capabilities helped me immensely in the research. I am very thankful to Dr. Suresh Kuiry for his kind cooperation and guidance throughout this research work.

I would also like to thank Dr. Yaw Obeng. His immense interest in research and high energy was highly motivational to me. I treasure his professional help as well as personal friendship. I am also thankful to Dr. Raj Vaidyanathan for valuable discussions and suggestions and also for serving as the thesis committee member and evaluating this thesis. I am grateful to Florida I-4, PsiloQuest, DOE, DOD, SBIR phase 1 and 2, Advanced Material Processing and Analysis Center (AMPAC), and Mechanical, Materials and Aerospace Engineering for providing financial support. I thank Materials Characterization Facility (MCF) at UCF for offering the characterization facilities required for conducting this research work. I would like to thank Karen Glidewell for her help.

I would also like to thank Surendra, Dr. Satyajit Shukla and Vish for their help in this work. I thank my personal friends like Vikram, Swanand, Chandra, Nidhi, and Sachin for all their help and support. I would also thank all the colleagues in the Surface Engineering and Nanotechnology Facility (SNF) laboratory for their cooperation.

I would also like to thank my brother Abhijit and sister-in-law Prajakta for their encouragement and support. Finally, I would like to thank my parents and sister for their endless love and support.

TABLE OF CONTENTS

LIST OF FIGURES	xi
LIST OF TABLES.....	xv
CHAPTER 1. INTRODUCTION	1
1.1 Copper (Cu) in Electronic Industry.....	1
1.2 Need of Planarization.....	2
1.3 Cu and Low- <i>k</i> integration	3
1.4 Chemical Mechanical Polishing (CMP)	3
1.4.1 CMP Process.....	4
1.4.2 Dielectric CMP	6
1.4.3 Metal/Cu CMP	7
1.4.4 Shallow Trench Isolation (STI)	7
1.5 Materials Challenges in CMP	8
1.5.1 CMP Pads.....	8
1.5.2 CMP slurry Design	9
1.6 Objective of this Study.....	11
1.7 Organization of the thesis	12
CHAPTER 2. BACKGROUND	15
2.1 Chemical Aspect of Cu CMP.....	15
2.1.1 pH.....	15

2.1.2	Oxidizers	16
2.1.3	Complexing Agents	19
2.1.4	Inhibitors	19
2.2	Pads	21
CHAPTER 3. EXPERIMENTAL		26
3.1	Specimen Preparation	26
3.2	Buffer Solution Preparation	28
3.3	Static Dissolution Study	28
3.4	Electrochemical Measurements	29
3.5	X-ray Photoelectron Spectroscopy	31
3.6	Secondary Ion Mass Spectroscopy	32
3.7	Fourier Transform Infrared Spectroscopy (FTIR)	33
3.8	Nanoindentation	33
CHAPTER 4. RESULTS AND DISCUSSION		36
4.1	Chemical Aspects	36
4.1.1	Dynamic Polishing Studies	38
4.1.2	Dissolution Characteristics	39
4.1.3	Electrochemical Polarization Behavior	51
4.1.4	X-ray Photoelectron Spectroscopy (XPS) analysis of Cu surface	55
4.1.5	Secondary Ion Mass Spectroscopy Analysis	62
4.2	Surface Modification of Application Specific Pads (ASP)	72
4.2.1	Secondary Electron Microscopy (SEM)	73
4.2.2	X-ray Photoelectron Spectroscopy	73

4.2.3	Fourier Transform Infrared Spectroscopy	82
4.2.4	Nanoindentation	84
4.2.5	Correlation of ATR-FTIR, XPS and Nanoindentation Results	90
4.2.6	Impact of Pad Surface Modifications on Polishing Performance	90
CHAPTER 5. CONCLUSION.....		92
CHAPTER 6. IMPACT OF CURRENT RESEARCH AND FUTURE TRENDS IN METAL CMP		94
APPENDIX: PUBLICATIONS.....		98
LIST OF REFERENCES.....		100

LIST OF FIGURES

Figure 1. Schematic of Chemical Mechanical Polishing	5
Figure 2. SEM micrographs showing cross sections of application specific pad (ASP) (left) and Rodel's IC1000/Suba IV stacked pad (right).....	25
Figure 3 . Schematic diagram of a low temperature RF Plasma Set-up.	27
Figure 4. The Electrochemistry Setup for the Cu dissolution.....	30
Figure 5. Cu-H ₂ O Pourbaix diagram.	37
Figure 6. Dynamic polishing on Cu wafer at various pH values.	40
Figure 7. Comparison of various inhibitor efficiencies using dynamic polishing Studies.	41
Figure 8. Effect of H ₂ O ₂ content on the dissolution rate of Cu in solution containing 0.1M glycine at (a) pH 2, and (b) pH 4.	43
Figure 9. Effect of glycine content on the dissolution rate of Cu in solution (a) 5% H ₂ O ₂ at pH 2, (b) 2.5% H ₂ O ₂ at pH 2, and (c) 2.5% H ₂ O ₂ at pH 4.....	45
Figure 10. Effect of benzotriazole content on the dissolution rate of copper in solution containing 0.1M glycine at pH 2 with 2.5% and 5 % H ₂ O ₂	46
Figure 11. Effect of benzotriazole content on the dissolution rate of copper in solution at pH 4 containing 2.5% H ₂ O ₂ and 0.1M glycine.	47
Figure 12. Effect of pH and H ₂ O ₂ content on the inhibition efficiency of benzotriazole (BTA) on copper dissolution in solution containing 0.1M glycine (a) 5% H ₂ O ₂ at pH 2, (b) 2.5% H ₂ O ₂ at pH 2, and (c) 2.5% H ₂ O ₂ at pH 4.....	48

Figure 13. Potentiodynamic polarization plots of copper in solution at (a) pH 2; (b) pH 2 with 0.1M glycine; and pH 2 with 0.1M glycine and H ₂ O ₂ content of (c) 2.5%, (d) 5%, (e) 7.5%, and (f) 10%.	52
Figure 14. Potentiodynamic polarization plots of copper in solution at pH 2 with 0.1M glycine (a) without H ₂ O ₂ , (b) 5% H ₂ O ₂ , and (c) 5% H ₂ O ₂ with 0.01M BTA.	53
Figure 15. Peak-fitted Cu (2p) XPS spectra from surface of copper immersed for 10 minutes in solution at pH 2 (a) 5% H ₂ O ₂ (b) 5% H ₂ O ₂ with 0.1M glycine, and (c) 5% H ₂ O ₂ , 0.1M glycine with 0.01M benzotriazole [1. Cu ⁰ , 2. CuO, 3. Cu-glycine complex, and 4. Cu-BTA complex].	58
Figure 16. Peak-fitted XPS N(1s) spectra from surface of copper immersed for 10 minutes in solution at pH 2 containing 5% H ₂ O ₂ and 0.01M glycine (a) without benzotriazole, and (b) with 0.01M benzotriazole.	61
Figure 17. SIMS depth Profile of Cu-wafer after immersing in solutions at pH 4 for 15 min containing (a) 2.5% H ₂ O ₂ , and (b) 2.5% H ₂ O ₂ and 0.1M Glycine.	63
Figure 18. SIMS depth profile on the copper surface after treating with pH 2 solution with 0.1M glycine and 5% H ₂ O ₂ (a) Cu, (b) -NH ₂ CH ₂ , (c) Glycine, and (d) Cu(H ₂ NCH ₂ COO) ⁺ .	64
Figure 19. TOF-SIMS spectra on (a) glycine; (b) D-glycine powder.	67
Figure 20. Static SIMS spectrum from the copper surface after treating in pH 2 solution with and 5% H ₂ O ₂ , 0.1M glycine and 0.01M BTA. Peaks identified at 1. CN ⁻ , 2. C ₃ N ⁻ , 3. C ₆ H ₄ N ⁻ , 4. C ₆ H ₄ N ₃ ⁻ 5. [(Cu ⁺) (C ₆ H ₄ N ₃ ⁻) ₂].	68

Figure 21. Static SIMS spectrum from the copper surface after treating in pH 4 solution with and 5% H ₂ O ₂ , 0.1M glycine and 0.01M BTA. Peaks identified at 1.CN-, 2.C ₃ N-, 3.C ₆ H ₄ N- 4.C ₆ H ₄ N ₃ - 5.[(Cu+)(C ₆ H ₄ N ₃ -) ₂].	69
Figure 22. Secondary Electron Microscopy images of ASP (a) uncoated; (b) Coated.	74
Figure 23. Chemical formula of the polymeric pad.	75
Figure 24. Deconvoluted XPS C (1s) spectra from the ASP surface after PECVD-TEOS treatment for (a) 10min, (b) 20min, (c) 30min, (d) 40min, (e) 45 min. possible peak identification: 1. C-C/C-H, 2. C- O, 3. carbamide, 4. C-Si.	77
Figure 25. Peak fitted XPS Si (2p) envelop taken from the ASP after TEOS deposition for (a) 10 min, (b) 20 min, (c) 30 min, (d) 40 min, and (e) 45min. possible peak identification: 1. Si-O, 2. Silicate, 3. Si-N, and 4.Si-C.	78
Figure 26. Variation in surface silanol / silcates in PECVD-TEOS coating as a function of deposition time.	79
Figure 27. Transmittance plot of surface ATR-FTIR signal through TEOS coated polyethylene-ethylene vinyl acetate (PE-EVA) foam substrate as a function of coating time.	83
Figure 28. Load-penetration behavior of CMP pads during nanoindentation on pad PECVD treated for 45 min. Inset: The slope change at the transition point at a depth of h _{tr} .	86
Figure 29. Variation of transition depth (h _{tr}) as a function of PECVD-TEOS coating time during nanoindentation tests. ⁹¹	87
Figure 30. Hardness as a function of PECVD-TEOS coating time. ⁹¹	88
Figure 31. Elastic modulus as a function of PECVD-TEOS coating time. ⁹¹	89
Figure 32. Correlation of relative blanket tungsten removal rate (W-RR) and PECVD-TEOS coating time.	91

Figure 33. Impact of current research on chemical mechanical planarization industry. 96

LIST OF TABLES

Table 1. List of different oxidizers used in the CMP Slurry.....	18
Table 2. E_{corr} , I_{corr} , and the polarization resistance (R_p) estimated from the polarization studies on copper in various solutions.....	56
Table 3. Variation of composition of XPS C(1s) envelope as a function of PECVD treatment time with TEOS on the top surface of ASP pads.....	80

CHAPTER 1. INTRODUCTION

1.1 Copper (Cu) in Electronic Industry

Ever since the first commercialization of the microchip there is a relentless drive in semiconductor industry to design smaller. As device manufacturers continue to follow Moore's law¹, increased performance requires the introduction of new materials.

Cu is widely used in the electronics industry for many years. It has been used for wiring and interconnecting material for long time. But actual transformation of the Cu usage from macro to micro electronics occurred after announcement of IBM in 1997 that Cu would be used in next generation of advanced IC chips, this has intensified Cu metallization effort at major IC manufactures.^{2,3} Slowly Cu started replacing aluminum (Al) and its alloys as interconnecting material due its properties like lower electrical resistivity and higher resistance to electromigration^{4,5}. Incorporation of Cu in the integrated circuit (IC) industry reduces wiring resistance and improves the reliability; however, it brings new challenges due to following reasons⁶

- Introduction of Cu by replacing Al makes wafer manufacturing more complex and relies on new and multiple technologies.
- Need for new patterning techniques
- Need for barrier layer, to reduce the diffusion of Cu but at the same time this raises several manufacturing issues like need of new manufacturing process.

- Need for the stringent process control since incorporation of any impurity hinders the conductivity of copper.

Incorporation of the copper in the IC metallization requires new patterning strategies, from which need for planarization has been generated.

1.2 Need of Planarization

Current ULSI technology enables chip to have few millions of transistors. Advances in the interconnection technology have played a key role in the continued improvements in the integrated circuit density, the performance and the cost per function. Continuing advances in the interconnection technology are seen as essential to the continued improvement in the IC performance⁷. The recent introduction of the Cu metallization, dual damascene processing, and fully articulated hierarchical wiring structures, along with the imminent introduction of low-dielectric-constant insulating materials indicate an accelerating pace of the innovation. In multilevel metallization, planarity is achieved by the extensive use of the chemical mechanical polishing (CMP). The IC Industry is heading towards the 50 nm node size and the planarization becomes the key issue in the success of the advanced semiconductor devices⁸.

There are two broad categories of planarization: local and global. The local planarization, i.e. an area with a high density of structures to be planarized, is made up of a high frequency of the high and low topography and is typically easiest to planarize. Global planarization, i.e., planarization of all structures across the chip to the same level, is far more difficult to achieve³. Beyond local and global planarization, the ability to uniformly remove the material being planarized is critical to final wafer planarization quality. In the recent years, the integration of the Cu with low k materials became a key issue for planarization.

1.3 Cu and Low-*k* integration

To reduce the parasitic electrostatic coupling and the propagation delays on chip, low *k* dielectric materials have been introduced in IC industry². Advantage of integration of low *k* material with Cu has improved device performance, at the same time; many design changes and process changes are involved. Different materials such as fluorinated glasses, silsesquioxanes, organosilicate glasses, polymers, and fluorinated polymers are slowly replacing conventional silicon oxide. ITRS mentioned that these low-*k* (2.0-2.2) range causes incorporation of porosity. Porous materials have many additional challenges for successful processing and integration. These materials are extensively evaluated for effective dielectric constant, the water absorption, the chemical reactivity, the temperature stability, and most importantly the compatibility of each material with the Cu metal and the barrier materials⁹.

1.4 Chemical Mechanical Polishing (CMP)

The name “Chemical Mechanical Planarization” alludes to the fundamental nature of the process. CMP is designed to advantageously use the chemical reaction and the mechanical energy in combination for global planarization. The use of CMP technique is not unique in planarization³. CMP process was historically used for polishing glasses, but IBM was the first company, which successfully implement this process in the IC manufacturing². Semiconductor industry starts using this process for wafer manufacturing since then. High degree of flatness with less material removal, gives CMP a cutting edge over other the processing techniques.

1.4.1 CMP Process

A typical CMP process setup has been shown in Figure 1. As shown in the figure, the wafer to be processed is held in the wafer carrier. Small portion of the wafer protrudes which comes in contact with the slurry and the pad. Polishing polymeric pad is held on the polishing platen. Pressure is applied normal to the pad surface through the polishing arm to the wafer. As shown in figure 1; a membrane or flexible carrier film is located beneath the wafer; the main function of this membrane is to distribute uniformly the applied pressure to all points on the wafer surface. Slurry used in the CMP process not only provides chemical reaction but also forms a layer between the pad and the wafer for fluid shear.

A detailed idea about the chemistry and the mechanics occurred at the interface of the wafer/slurry/pad is shown in Figure 1. Different chemicals and abrasive particles present into the slurry react with the sample. These particles allow easy removal of metal from the protruded areas.

In general, the CMP consumables such as polishing pad and slurry play key role in the process. Input of the process is varied by varying the parameters of these consumables. These variables are manipulated in order to obtain the optimum process result.

Several factors need to be considered to describe the CMP process. The important factors are¹⁰

- Structure and composition of the surface to be polished.
- Formulation of slurry.
- Mechanical and surface properties of Pad.
- The relative speed between the pad and the wafer

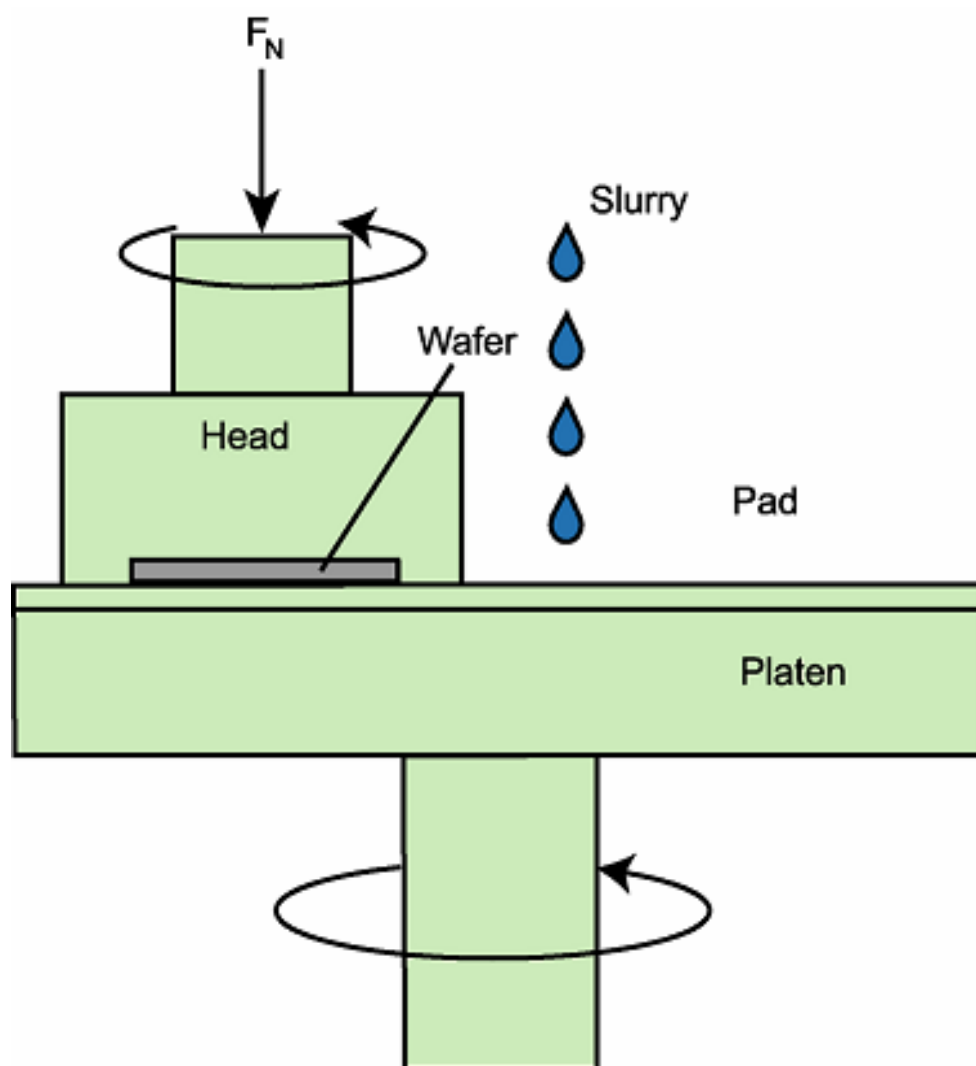


Figure 1. Schematic of Chemical Mechanical Polishing

- Applied pressure to the wafer.
- Temperature.
- Porosity and grooves on the pad which helps in the fluid flow on the pad.

Major advantage of the CMP process is global planarity for multilevel, sub 0.5 micron metallization schemes can be achieved easily. Also, CMP is one step process which reduces the processing cost as well as the time. All type of the surfaces can be planarized, provides alternate means of the patterning metals, improves metal step coverage and subsequently the interconnect structure. Main advantage of the CMP is the reduction in the defect densities in processing of the wafer³.

At the same time high initial cost, exact formulation of the slurry chemistry and the requirement of post CMP cleaning are some of the major disadvantages of the CMP process¹¹.

Schemes are widely used in the planarization using CMP are dielectric CMP, metal CMP and Shallow trench Isolation (STI).

1.4.2 Dielectric CMP

Oxide CMP is one of the most widely used technique. It is the intermediate process after the initial interlayer dielectric (ILD) deposition and metal levels for planarization. This occurs by both chemical and mechanical mechanisms. Chemicals present into the slurry react with the dielectric materials, weakening the surface bonds allow easy abrasion of the materials^{2, 3}. Silicon Oxide (SiO_2) is the most widely used dielectric material in the CMP industry. Since it has been studied from last many years, CMP of SiO_2 is one of the most understood processes¹².

1.4.3 Metal/Cu CMP

The Cu CMP process involves the removing of Cu and the barrier over the field regions to define the interconnect^{13,14}. In the Cu inlay approach, the vias and the trenches have been created by patterning and etching dielectric layer. The diffusion barriers (like Tantalum) are lined in the vias and then Cu seed layer is deposited to ensure and initiate bulk Cu deposition. Various techniques have been used for bulk Cu deposition. Most popular techniques used for Cu deposition are the physical vapor deposition (PVD), the chemical vapor deposition (CVD) and the electrochemical deposition (ECD)³. The final step in the Cu inlay approach is removing of excess the Cu on surface using the CMP process.

One of the advantages of dual damascene Cu interconnects is cost saving due to the elimination of the manufacturing steps for every metal mask level compared to a typical Al interconnect strategy employing tungsten plugs. It is important to consider that cost saving is not sacrificed by the speed at which one can get the advanced chip.

Many challenges exist in developing an ideal Cu CMP process. The main process issues include the controlling of the extent of the Cu dishing and the inter-layer dielectric (ILD) erosion and controlling defects formed by CMP¹⁵. With the integration of Cu with low-k materials and use of the double damascene (DD)¹⁶ process increases the challenges of the Cu CMP process.

1.4.4 Shallow Trench Isolation (STI)

From the past few years CMP is widely used in the shallow trench isolation (STI) process¹⁷. The most basic steps in STI process includes silicon etch, oxidation, trench fill by the CVD and the CMP. Transition to the shallow trench isolation (STI) from localized oxidation of the silicon (LOCOS) is natural from the design standpoint. STI significantly shrinks the area needed to isolate the transistor while offering the superior latch up immunity, smaller channel

width encroachment and the better planarity. From processing point of view, however, the transition to the STI is little more complicated¹⁸. The greater challenges lie in providing void-free, seamless gap filled by CVD and subsequent uniform planarization by CMP.

1.5 Materials Challenges in CMP

For an average Cu CMP process, the cost of the consumables is between 50-70% of the overall process¹⁹. CMP consumables play major role in obtaining optimum yield from the process. Pads and slurry are the two major consumables, on which most of the research has been focused. At sub 0.1 micron regime, the key challenges in the CMP process are mentioned below¹⁰:

- Very small amount of materials to be removed: This needs effective planarization with very small polishing rate. High precision and process control is needed.
- Nature of the finished surface: Surface planarized must be smooth enough. This dominates the performance and the reliability of the overall process.
- Quality Control: Since planarization area is about submicron level defect free and errorless process needed.
- Chemical attacks: Material should not get any kind of galvanic corrosion as well as corrosion due to chemicals present into the slurry.

1.5.1 CMP Pads

Polishing Pads are the major consumables affecting critically the within-wafer non-uniformity (WIWNU) and wafer-to-wafer non-uniformity (WTWNU) in the planarization technology²⁰. Role of the CMP pad is one of the key aspects in the CMP process.

CMP pad is made up of one or more of polymeric materials. Typical role of CMP pad include³:

- Provides support against the wafer surface, allowing the wafer surface to experience the impact of the mechanical and the chemical forces leading to material removed.
- To transport abrasive containing and active slurry for the chemical action.
- To transfer the load to the work piece surface.
- Wear and exposure of the new open cell of the polymeric material on surface by conditioning.

The mechanical properties and the surface morphology of the pads play important role in governing the overall CMP process. Ideally, to obtain a planar surface, one should have a rigid and inert pad surface that can carry abrasives and the chemicals present in the slurry¹⁰. But in reality the pad is not a rigid as well as chemically inert material. The chemical present in the slurry changes the surface or the bulk chemistry of the pad, while due to mechanical abrasion wear of the pad takes place. Since pads get affected by the chemicals present in the slurry, exact designing and formulation of the slurry is important.

1.5.2 CMP slurry Design

The main function of the slurry used in the Cu CMP process is to facilitate easy removal of Cu by both chemical and mechanical action through abrasives present in the slurry³. It also acts as a lubricating media between the pad and the wafer. Excellent performance for a Cu polishing process required intelligent mixing and use of significant independent slurry components. In CMP, slurry additives further increase the equipment costs¹⁹.

Slurry constitutes of different chemical components such as oxidizers, inhibitors, complexing agents, surfactants and the abrasive particles. Unlike oxide CMP, slurry formulation

is the difficult task in the Cu CMP since in the oxide CMP major emphasis is to obtain the global planarization. Slurry chemicals affect primarily the chemical component, e.g. etch rate. On the basis of their role in the process, CMP slurries can be classified into two major categories¹⁹: (a) Cu polish slurry and (b) barrier slurry. While the Cu slurry market is by no means established, it is the mainstay of the polish process as it accounts for the bulk Cu removal.

The cost considerations have also led several IC device manufacturers to develop the Cu slurries that are adapted to their respective integrations, thereby achieving the requisite process performance along with the reduced costs and the formulation of the slurry is one of the major aspects of CMP research work. While etching the Cu, it also affects the properties of the pad, film and the abrasive surfaces. Therefore, overall polishing performance gets affected indirectly. There are different slurries used at different manufacturing steps. Initially slurry having high concentration of oxidizing agents and abrasive particles is used; while at the end stages of manufacturing abrasive free slurry is preferred to avoid the scratching of the end product²¹. The commercial slurry manufacturers have identified the Cu CMP slurry as a growth market and continue to focus their efforts towards improving the manufacturability of the Cu CMP slurries. Some typical characteristics of the slurry are mentioned below³:

- Most important characteristic of slurry is that various chemicals present in the slurry should not react with each other.
- Slurry should have good shelf life.
- Slurry should provide high Cu dissolution rate at the protruded regions while it should protect the metals in the recesses and most importantly at the same time desirable output should be obtained.

- Chemicals present in the slurry should not react and deteriorate the polishing pad used during the process.
- Abrasive present in the slurry should be well suspended and stable. Maximum size of the abrasives should not exceed 500 nm to avoid any scratching of the wafer.
- Slurry should have good colloidal stability.
- Abrasive present in the slurry sometimes get adhered to the wafer surface due to the electrostatic interaction. Removal rate variation from center to edge of the wafer must be very little.
- Excessive pitting of the material which is removed from the wafer is avoided.

1.6 Objective of this Study

Formulation of slurry with exact concentration of the oxidizers and the inhibitor concentration is one of the important parts of the CMP research. In the present investigation work is carried out to understand the effect of hydrogen peroxide (H_2O_2) as an oxidizing agent, the effect of glycine as a complexing agent. Detail studies have been carried out to understand the presence of glycine in pH 2 and H_2O_2 solution. Formation of the Cu-glycine complexation and the enhancement of the dissolution rate are explained thermodynamically. Effect of addition of BTA, formation of the polymeric film on the Cu surface and suppression of the Cu dissolution rate are explained in detail. Different techniques like XPS and SIMS are extensively used for surface characterization of the Cu surface in light of effective Cu-CMP.

Another objective of the present study is to use plasma enhanced chemical vapor deposition (PECVD) for modification of the surface of the application specific pads and the formulation of exact slurry chemistry in order to have better polishing characteristics for the

chemical mechanical planarization (CMP). Enhancement of the wear resistance of the polishing pads is also one of the parameters to be enhanced by plasma treatment. A post plasma treatment can also be given to enhance the surface properties of the pad surface. The extent of the nanoscale surface (10-50 nm) properties enhancement is also to be studied with the help of XPS. The morphology of the surface structure was studied using SEM. Nanoindentation technique has been used to evaluate mechanical properties of the pad surface in collaboration with Dr. Vaidyanathan's research group. This research is a step to engineer suitable pad materials for solving many queries in CMP process.

1.7 Organization of the thesis

Optimization of the slurry and the polishing pad properties are essential in improving the overall CMP process. Exact formulation of the slurry and investigation of the pad's microstructure, the surface and the mechanical properties can further elucidate the overall performance of the polishing process. Although several studies has been done on this area, the aim of this study to optimize critical CMP process parameters in designing effective slurries and pads on the basis of basic knowledge of this field.

This thesis is divided into six chapters. Chapter 1 gives idea of need of CMP process and gives idea about the basics of CMP.

Chapter2 the literature, related to formulation of slurries and pads, is reviewed, in detail. The fundamentals of the Cu dissolution, the need of high dissolution slurries, and the requirement of inhibitors into the slurries are discussed. Also the literature regarding the surface and the mechanical properties of pad, chemical attack of the different chemicals present into the slurries on the pad surface and wear and erosion of pad surface are considered in this chapter.

The need for the development of the new generation pad and the use of surface modification technique for the improved performance of the polishing pad is also taken into consideration in this chapter.

Chapter 3 gives an idea about the different experimental techniques used for the characterization of the slurry and the CMP pad. Typical static dissolution rate and electrochemical studies give an idea about the occurrence of the highest dissolution rate of Cu. XPS and SIMS analysis indicates the different chemical states present on the Cu surface. It is also helpful in determining the complex formation of Cu with various components present into the slurry. In this current research work XPS analysis is extensively used for conducting the surface modification of the polishing pads. Moreover, FTIR and nanoindentation techniques have been used in the pad surface analysis.

Chapter 4 is divided into two sections 1. Chemical aspect of Cu CMP and 2. Surface modification of application specific pads. First section covers the results obtained from different techniques used as mentioned above and further correlation for optimizing different slurry parameters such as oxidizers, inhibitors and complexing agents in regard to CuCMP. It explains in-detail the mechanism of the oxide formation as well as Cu-glycine and Cu-BTA complex formation in detail. Second part of this chapter covers the effect of the surface modification of CMP pad, in detail. XPS analysis of the pad surface has been done to understand the performance of the pad with respect to the TEOS deposition time and relate to the pad surface modification. Results obtained from the XPS analysis of the pad surface are supported by Nanoindentation and FTIR analysis. Over all effect of the surface modification on polishing performance has been discussed in this chapter.

Chapter 5 summarizes the overall results and further concludes the current CMP research.

Chapter 6 gives an idea about the future trend in the CMP industry which includes application of nanocrystalline materials to the CMP, is discussed briefly, and will be the part of future research.

CHAPTER 2. BACKGROUND

2.1 Chemical Aspect of Cu CMP

Cu CMP slurry is one of the most expensive chemical costs in the semiconductor manufacturing. Since it constitutes the major cost of the overall process it is the challenge of the process engineer to select the proper slurry which best fit the rigorous requirements for the device being built. To a great degree, the selection of the slurry with specific capabilities determines the polishing performance and capabilities that can be achieved by the polishing system. With integration of the low-k materials with Cu and sizes of the features scaling towards few nanometer scale, designing of the slurry for polishing Cu and barrier layers at the same time achieving the desired dishing and erosion values is unlikely¹⁹. At the same time, removal of the slurry from the surface without leaving any macroscopic, microscopic, or electrically active defect is very important.

Various slurry constituents to be considered while designing slurry are listed below:

2.1.1 pH

One of the most important parameters to be consider while slurry is formulated. It directly affects^{22,23} the dissolution rate and solubility of the metal (here Cu) to be polished. On the basis of the studies of the pourbaix diagram of material to be polished, pH of the slurry is decided. pH of the slurry also important for abrasive suspension. It directly affects the stability

and effectiveness of the abrasives³. Since slurries directly come into contact with the pad it also affect the pad morphology as adhesives used for bonding pad on the platen.

Huang *et al.*²⁴ shows the effect of pH on the dissolution rate in case of hydroxylamine as an oxidizing agent. Dissolution rate increases till pH value 6 then at higher pH values the dissolution rate gets suppressed. Also Seal *et al.*²⁵ recently reported the oxidation, dissolution and modification of the Cu surface by addition of H₂O₂ as oxidizing agent and glycine as complexing agent in pH 4. Present study in strongly acidic media is motivated by the industrial trend towards using acidic slurries for bulk Cu CMP in attempts to minimize the possibility of de-lamination at the metal-low-k dielectric interface. It allows planarization at relatively low down-forces and table speeds. The use of the acidic slurries emphasizes the chemical aspects of CMP due to the active dissolution of Cu in strong acids.

2.1.2 Oxidizers

Chemical reactions that occurred during the Cu CMP process are electrochemical in nature and oxidizers play very important role in the chemical reactions. By raising the oxidation state of metal either by oxidation or reduction reaction it helps in active dissolution or formation of passive film on the surface can be achieved. In case of Cu CMP, the rate of dissolution is proportional to rate of reduction-oxidation reactions³. Kaufman's²⁶ proposed model of active dissolution of Tungsten (W) - CMP does not validate for the Cu CMP process. But Steigerwald *et al.*²⁷ performed active studies on the Cu dissolution using various chemicals and states that Cu does not dissolve just by forming the oxide film on the surface, but dissolution of Cu is a two step process which involves abrasion of Cu in initial step. Active dissolution of the abraded Cu in the slurry by chemical action is followed.

The use of sodium chlorate $[\text{NaClO}_3]^{28}$, Hydrogen peroxide $[\text{H}_2\text{O}_2]^{23,29,30,31}$, and Iron nitrate $[\text{Fe}(\text{NO}_3)_3]^{28}$ as oxidizers during CMP was attempted in previous studies. Different oxidizers used in the CMP industry are listed in Table 1.

Amongst all the oxidizers presented in the table, H_2O_2 and hydroxylamine are the most popular oxidizing agents in CMP industry since they required minimal post CMP cleaning. Furthermore unlike the iodate and ferric ions, they do not leave any trace of oxidizers and reduction product on the wafer. H_2O_2 shows very anomalous behavior as an oxidizing agent. For number of years research has been conducted on the radical formation due to the presence of hydrogen peroxide. In most studies it has been observed that polishing rate initially increases and then decreases with increasing concentration of H_2O_2 into the solution^{32,33}. Steigerwald *et al.* in detail studied the effect of HNO_3 and NH_4OH and they further mentioned that with increasing the concentration of these oxidizers (nitrate ions) dissolution rate increases linearly. Similar results were found in the literature.^{34, 35}

Though H_2O_2 slurries are important in the Cu CMP process; they have not been investigated adequately. The literature explained the drop in the dissolution rate as a result of oxide layer formation. But it fails to explain the oxide layer formation under unfavorable conditions and how this oxide formation is linked to the H_2O_2 concentration.

In the present study, the effect of the variation of the concentration of H_2O_2 on the Cu surface has been carried out.

Table 1. List of different oxidizers used in the CMP Slurry.

Oxidizing agents	Open Circuit Potential E^0 (V)
Ferric Ion $\text{Fe}^{3+} + \text{e}^- \rightarrow \text{Fe}^{2+}$	0.771
Ferricyanide $\text{Fe}(\text{CN})_6^{3-} + \text{e}^- \rightarrow \text{Fe}(\text{CN})_6^{4-}$	0.358
Hydroxylamine $\text{NH}_3\text{OH} + 2\text{H}^+ + 2\text{e}^- \rightarrow \text{NH}_4 + \text{H}_2\text{O}$	1.35
Nitrate Ion $\text{NO}_3^- + 2\text{H}^+ + 2\text{e}^- \rightarrow \text{NO}_2^-$	0.835
Iodate Ion $\text{IO}_3^- + 6\text{H}^+ + 6\text{e}^- \rightarrow \text{I}^- + 3 \text{H}_2\text{O}$	1.085
Chlorate Ion $\text{ClO}_3^- + 6 \text{H}^+ + 6 \text{e}^- \rightarrow \text{Cl}^- + 3 \text{H}_2\text{O}$	0.62

2.1.3 Complexing Agents

The main function of complexing agent is to form a soluble complex with Cu ions or abraded film material and improve the overall dissolution rate of Cu. An important balance between the mechanical removal rate from the surface being polished and the dissolution rate from the surface being polished and the dissolution rate can be achieved by selecting desired complexing agents. A numbers of complexing agents are available in the market but minimal post CMP cleaning requirement along with inertness for complex formation with the barrier metals are the main requirement for the complexing agent selection.

Glycine, ethelenediaminetetraacetic (EDTA) acid, and ethelenediamine (En) are some of the leading complexing agents used in the Cu CMP industry^{25,33}. Aksu *et al.* reported electrochemical studies of glycine, EDTA and En on Cu. They concluded that glycine shows highest efficiency as complexing agent as compared to other two. Studies^{25,33} shows that glycine in presence of hydrogen peroxide facilitates the active dissolution of Cu.

In the current studies, investigation were carried out to understand the effect on glycine in pH 2 and pH 4 solution in presence and absence of the hydrogen peroxide and the benzotriazole.

2.1.4 Inhibitors

For planarization of the uneven surface topography to occur, isotropic etching should be avoided. Higher dissolution rates remove Cu from both the protruding as well as the recessed region, resulting in poor planarization. In the presence of chemical content in the slurry like H₂O₂ and glycine dissolution of Cu in the recessed area is same as dissolution in the protruded area³⁶. In order to prevent the dissolution of the Cu in the recessed area corrosion inhibitors are added to the solution. Corrosion inhibitors form a passive film on the Cu surface and protect the

active dissolution. The following are some of the requirements that should be satisfied by the chemical to become an appropriate Cu inhibitor.³⁷

- The corrosion inhibitor get chemically adsorbed or chemically bonded to the Cu surface.
- It should form a complex with the Cu, in the form of polymeric film on the surface.
- This polymeric film should not be soluble in slurry.
- It should be stable at wide range of pH values. Since both acidic and alkaline both type of pH used in the slurry formulation. It should withstand at both the condition.
- Anodic areas are the central areas for the pitting corrosion; the inhibitor should act as an anodic inhibitor.
- It should not be harmful or hazardous to the user.
- To avoid any traces on the metal surface and to ease the cleaning procedure metallic inhibitors are avoided.
- The inhibitors should be non-toxic, non-hazardous and should be inexpensive
- It should be available in pure form.

Different chemicals are used in the Cu industry as corrosion inhibitors, such as 2-aminopyrimidine (AP), 2-amino-5-mercapto-1, 3, 4-thiadiazole (AMT), Benzotriazole (BTA), 2-mercaptobenzimidazole (MBI), 2-mercaptobenzothiazole, 3-amino-triazole (ATA). Faltermeier *et al.* did an exclusive study on Cu inhibitors and concluded that in all inhibitors BTA shows the highest efficiency as a corrosion inhibitor. Due to its perceived advantages and satisfactory results, BTA has been the predominant corrosion inhibitor used in the conservation of the Cu and its alloys. BTA is the most popular inhibitor used in the CMP industry but some conflicting data has been reported. Several studies^{30,38,39,40,41,42,43,44,45} have been carried out to understand the

inhibitive action of benzotriazole (BTA) on the Cu. It is observed that in the presence of BTA, Cu forms a Cu (I)-BTA complex. Walsh *et al.* extensively studied the geometry of the BTA - species on the Cu surface. In the presence of the H₂O₂, BTA and organic acids in the CMP slurry were found to be very effective in controlling the metal removal²⁵. However, Wang *et al.* reported a decrease in the rate of polishing with increased H₂O₂ content. Although BTA adsorption on the Cu₂O is well documented however there is still controversy exist over adsorption of BTA over oxide free Cu⁰ surface. This study gives an overview of the Cu-BTA complex formation in the presence of H₂O₂ and glycine in pH 2 and pH 4 solutions.

2.2 Pads

The polishing pad is one of the most important, and yet least understood parameter in the CMP system^{3, 10}. In the CMP process, the polishing process involves intimate contact between “high points” on the wafer surface and the pad in the presence of slurry. As discussed earlier, Cu dissolution mechanism involves removal of metal by shearing at the pad-wafer interface by abrasion action and the dissolution of the abraded material into the slurry chemicals. Since Cu removal from the surface occurred due to abrasion action; pads used in the Cu CMP process play key role in the overall process. The pad structure, mechanical as well as the surface properties are important in determining polishing rate and planarization ability of the process, therefore these are usually determined empirically. Direct correlation between the pad properties and the polish performance are limited in this field of study.

As pad is not a rigid material its properties changes as the chemical/solvent rigidity and wear. Chemicals present in the slurry mainly react with the pad material and due to which surface, as well as bulk, chemistry of the pad varies⁴⁶. It also affects the bonding between the pad and abrasives, and electrochemical effects. Pads are generally made up of polymeric materials which are spongy,

porous, absorb water and lead to the creation of dipoles near the surface leading to a charge state. Also due to polishing, surface properties experience the changes.

Several properties of the pad are to be designed and evaluated during the designing. The specific gravity, hardness, compressibility, surface roughness, and elasticity are some of the important properties of the pad. The heat and the mechanical energy are the primary causes of the polymer degradation⁴⁷. The chemical composition of the pad is decisive factor in the overall stability of the polymeric pad.

The elastic properties of the pad material significantly influence the rate of material removal and the final planarity⁴⁸. In general, the elastic properties are a function of both the intrinsic polymer and foam structure. Polyurethane-based pads such as IC1000/Suba IV have been used successfully to obtain both uniformity and efficient topography reduction, due to their unique property that combines high strength with hardness, bulk modulus and high elongation at break⁴⁹. However, the polyurethane pads showed a reduction in the material removal rates with polishing time which is attributed to the changes in the mechanical response of the pads under conditions of critical shear. The interaction of the pad and the polishing slurries^{50,51} has also contributed significantly to the functionality loss of the polyurethane-based CMP pads. An increasingly utilized method for improving the stability is the chemical modification of polymers. The polyurethane pads generally have around 35% of pores on the surface which need the reconditioning of the pad after some time of the wafer processing. The gross mechanical and the surface properties of the polyurethane pads depend on the molecular structure and the ingredients and unique supermolecular properties of the polymer. However, these polyurethane pads are incompatible with some of the chemicals used in Cu CMP, especially with H_2O_2 ⁵². Due to the chemical attack, pad surface get roughened and need of conditioning or pad change occurred frequently.^{53,54}

Recently, a new class of the application specific polishing pad (ASP) based on the thermoplastic polyolefin was developed by Obeng and Yokley⁵⁵ to overcome such incompatibility problems. The application specificity for the pad was accomplished by matching the micro-mechanical properties of the pad surface to the material being removed during CMP.

Pads can be surface modified with a soft ceramic coating using PECVD. The use of functional coating as one of the surface engineering approaches⁵⁶ has increasingly become an effective means for enhancing and modifying the mechanical and chemical properties of the pad surface. Advantages⁵⁷ of plasma treatment of the polymeric pads are:

- Elementary processes with high activation energies of several electron volts are possible in low pressure plasmas without elevated gas (ion, neutral) temperatures. There is almost no thermal load for sensitive polymer materials during low pressure plasma treatment.
- While the chemical structure of a shallow surface layer can be changed significantly, the bulk properties remain unchanged.
- An extreme wide range of surface modifications can be realized with different low pressure plasmas.
- The amount of toxic byproducts is low compared to wet chemistry.

Although polishing of the PECVD formed dielectric layers using usual polishing pad are routine in CMP^{58,59} investigation on the polishing behavior of PECVD modified pad is missing.

Scanning electron micrographs of the cross sections of such ASP3200 pad (Psiloquest Inc., Orlando, FL) and the standard IC1000/Suba-IV pad (Rodel Inc., Newark, DE) are shown in Figure 2. Although both pads are stacked-type, the ASP is distinguished by the presence of a soft ceramic-coated polyolefin foam layer on top of the hard condensed polyolefin sub-pad. Moreover, the

ASP3200 pad uses thermo-mechanical lamination instead of pressure sensitive adhesives to bond the top and the sub-pads together.

In the case of ASP pads, the coating modifies the viscoelastic properties of the soft polyolefin foam thereby tuning both the chemical and mechanical properties of the pad-wafer interface to match with those of the material being removed in the CMP process.

Consequently, it not only improves the polishing rate selectivity but also reduces the process induced defects such as scratching. Furthermore, the presence of metal-oxides on the top surface of the PECVD coated ASP pad makes the pad permanently hydrophilic, thereby, eliminating the mandatory storing of the pad under wet condition when these are not in polishing operation. The surface modification of the first generation ASP pads was accomplished through PECVD of various dielectric films, from organometallic precursors . The wear of the surface coating alters the polishing characteristics of the pad and limits the useful life of such first generation pads.

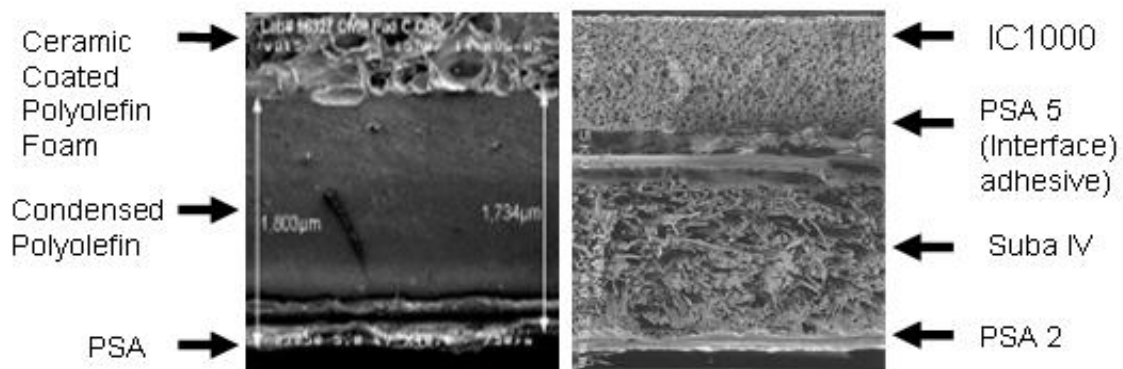


Figure 2. SEM micrographs showing cross sections of application specific pad (ASP) (left) and Rodel's IC1000/Suba IV stacked pad (right).

CHAPTER 3. EXPERIMENTAL

3.1 Specimen Preparation

All the experiments in the present study were carried out using 99.98% pure Cu foil (Sigma Aldrich Inc., Milwaukee, WI); with 2.5 cm × 2.5 cm in size and 1 mm thick. The Cu specimen was initially washed in a 10% hydrochloric solution to remove any native oxide from the surface, and dried in air stream. Hydrogen peroxide (30%) and benzotriazole is obtained from Sigma Aldrich while glycine and deuteriated glycine is obtained from Alfa Aker Inc.

Commercial polyethylene and ethylene vinyl acetate (PE-EVA) foam specimens were coated with PECVD-TEOS. Reaction chamber pressure was maintained at 200 mTorr. TEOS to oxygen ratio was 1:1. Details about specimen preparation and removal rate experiments are explained elsewhere . Large sheets of the substrate (PE-EVA) were coated as a function of time. All samples were dried in vacuum desiccators prior to analysis. All process had been done in a clean room to avoid human contamination of the sample surface.

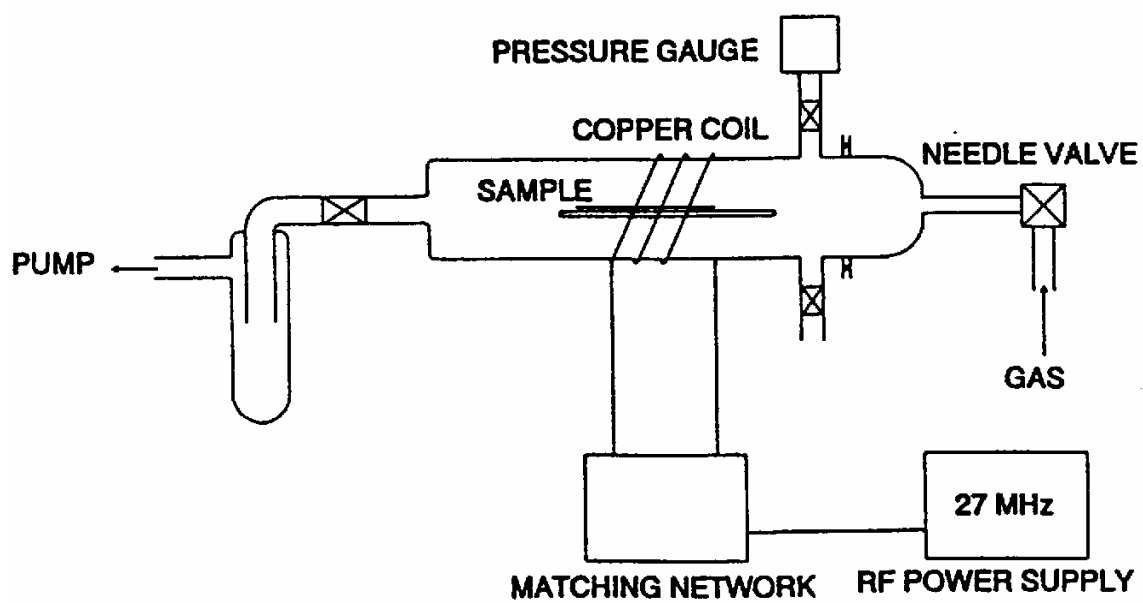


Figure 3 . Schematic diagram of a low temperature RF Plasma Set-up.

3.2 Buffer Solution Preparation

Buffer solutions were prepared in the laboratory as per the procedure available in the literature⁶⁰. For 100 ml of pH 2 buffer solution, 6.5 ml of 0.2 M HCl solution and 25 ml of 0.2 M of potassium chloride were mixed, and the solution volume was made to 100 ml by adding de-ionized (DI) water. In order to prepare 100 ml of pH 4 buffer solution, 50 ml of 0.1 M potassium hydrogen phthalate and 0.1 ml of 0.1M HCl were mixed and the solution volume was made up to 100 ml with the addition of DI water. The pH values of the solutions, thus prepared, were measured using a pH meter (Denver Instrument; Model 250).

3.3 Static Dissolution Study

Dissolution experiments were carried out in a 200 ml glass beaker with 100 ml of polishing solution to find out the static etch rates. The Cu specimen was initially washed in a 10% hydrochloric solution to remove any native oxide from the surface, dried in air stream and weighed in a microbalance (Sartorius; Model LA230P; ± 0.01 mg). Subsequently, it was immersed in the test solution for ten minutes. After immersing for a specified time of 10 min, the Cu specimen was taken out, washed in de-ionized water, dried in air stream and mass of the sample were taken again. The dissolution rate or static etch rate was calculated from the average mass loss data of three such identical experiments. Static etch rates in $\text{nm}\cdot\text{min}^{-1}$ of a Cu sample for this slurry were estimated as a function of hydrogen peroxide concentration with 0.1 M glycine. Dissolution study was also conducted as a function of glycine and BTA concentration variation in 2.5% and 5% H_2O_2 solutions.

3.4 Electrochemical Measurements

Potentiodynamic polarization tests were carried out to study the passivation and dissolution behavior of Cu surface in various solutions. Cu foils were first polished with sandpaper (Grit 180 and Grit 1200) and washed in 10% hydrochloric solution to remove any native oxide from the surface and dried in air stream. Polarization experiments were performed with an EG&G Princeton Applied Research (Model 273) potentiostat/galvanostat to obtain the polarization plots. An EG&G Princeton Applied Research Model 352 Softcorr TMII corrosion software was used to control the potentiostat/galvanostat. An EG&G corrosion flat cell (Model: K0235) consisting of three electrodes, namely a platinum counter-electrode, the Ag/AgCl reference electrode and a Cu sample as working electrode, was used for the investigation. The reference electrode was inserted into the corrosion cell through a lugin bridge whose tip was at a distance of 2 mm from the working electrode. The voltage scan rate was used at 0.1mV/s.

Typical setup used for the electrochemistry studies has been shown in figure 4.

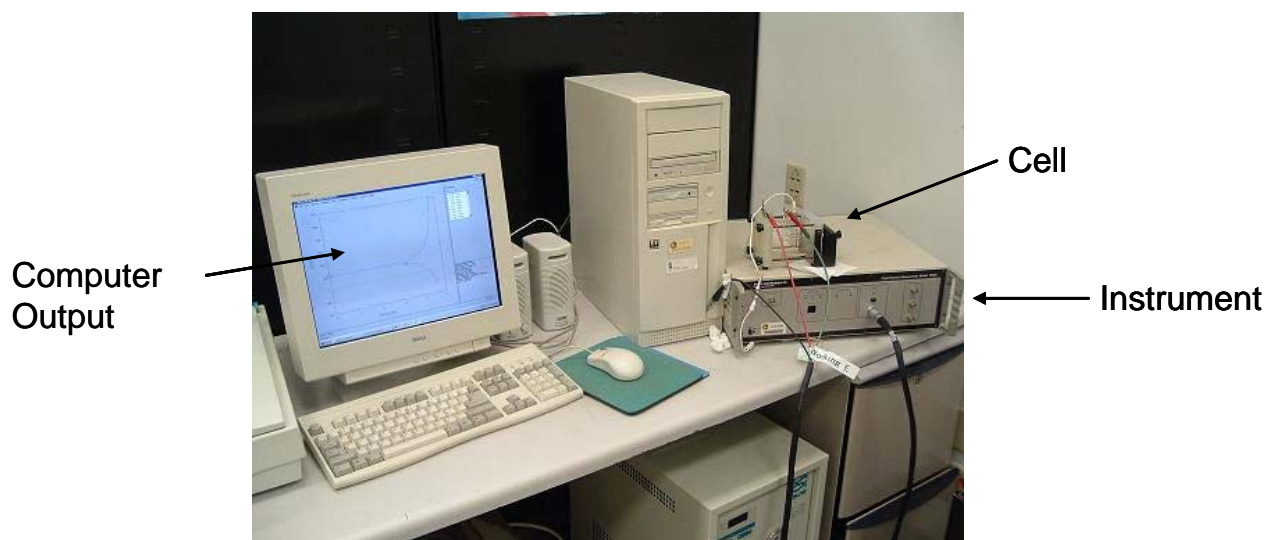


Figure 4. The Electrochemistry Setup for the Cu dissolution.

3.5 X-ray Photoelectron Spectroscopy

The surface modification of Cu specimens in various solutions of glycine and H₂O₂ and BTA, as well as the surface modification of the pads for different deposition time of TEOS, were characterized using a PHI 5400 X-ray photoelectron spectrometer at a base pressure of 10⁻⁹ Torr. Cu specimens were dipped in the requisite solution for specified time and then it was taken out and dried in inert atmosphere. Although care was taken to minimize the exposure time in air, the atmospheric exposure could not be avoided completely as the experiments were not performed in a glove-box. For surface analysis of pad sample a small piece of size 1 cm x 1 cm cut from the each coated sheet.

Subsequently the specimen was inserted in the XPS high vacuum chamber. The spectrometer was calibrated using a metallic gold standard [Au (4f_{7/2}): 84.0 ±0.1eV]. Non-monochromatic Mg K_α X-ray source with energy of 1253 eV at a power of 250 W was used for the Cu surface analysis. Power of 150 W and 15 kV was used as experimental conditions for pad surface analysis. Charging shifts produced by the Cu sample were removed by using a binding energy scale referenced⁶¹ with respect to the C (1s) binding energy of the hydrocarbon part of the adventitious carbon line at 284.6 eV. While charging shift produced by polymer sample were removed by using binding energy scale referenced with respect to the C (1s) binding energy of hydrocarbon part of adventitious carbon line at 285.0 eV⁶².

Elements present were identified from the survey spectra. And for further analysis high resolution spectra were recorded from the individual peaks at 30 eV pass energy.

The relative surface atomic concentration was calculated using the following relation⁶³ :

$$\frac{N_O}{N_{Si}} = \frac{I_O \sigma_{Si}}{I_{Si} \sigma_O} \quad (1)$$

Where, N_{O} and N_{Si} are the number of oxygen and Si atoms per cm^3 of the specimens, respectively. The terms I_{O} and I_{Si} are integrated intensities under oxygen and silicon peak, respectively. The terms σ_{O} and σ_{Si} are atomic sensitivity for oxygen and silicon, respectively. The values of σ_{O} and σ_{Si} were obtained from the literature for stoichiometry calculations as 0.66 and 0.25, respectively. Elemental ratios were then used to compare samples from varying treatment conditions.

Individual C (1s), O (1s) and Si (2p) peaks were deconvoluted using specialized peak fitting software and procedure described in the literature. As shown in the results section, this enabled the determination of the functional group present on the pad and the chemical states of the Cu surface. Before deconvolution each peak is smoothed using Savitzky-Golay algorithm. This is a time domain procedure that fits a fourth order polynomial in a moving window of a sizable number of data points. Once the data is smoothed a baseline which is best suited for given data is chosen. A Gaussian-Lorentzian sum function is used to fit the individual peak in the deconvolution. The percentage of overall area contributed by each individual peak can then be determined. Due to the exposure of the samples to the X ray source degradation of the sample, outgassing or dehydration of sample occurred and this can be successfully overcome by in-situ cooling using liquid Nitrogen.

3.6 Secondary Ion Mass Spectroscopy

Secondary Ion Mass Spectrometry (SIMS) data under static condition were collected using ADEPT 1010 system from Physical Electronics Inc. This instrument is capable of operating over a wide range of beam energies: 250eV to 8 KeV for oxygen and 250eV to 11 KeV for Cesium⁶⁴. It also offer full elemental coverage, sub-ppm range sensitivity for most of the elements, and a spatial resolution of less than 5micron.

In current studies ion gun operated with a 3kV oxygen beam at 60 degree off the specimen normal. For all data acquisitions, a beam of 3 pA was rastered over an area of 250 μm

square. The analysis was carried out from the signal coming from the central 30% of the sputter crater area.

3.7 Fourier Transform Infrared Spectroscopy (FTIR)

FTIR was run on a Perkin-Elmer System spectrum 1 with KBr detector, and equipped with a Series-I FTIR Microscope (ZnSe detector). The system has a spectral range from 6000 to 250 cm^{-1} . The Image software package allows rapid scanning of large specimens. Attenuated Total Reflectance (ATR) kit used along with the FTIR instrument for the surface studies of the pad. A small sample of size 1" x 1" is used for the FTIR analysis. The sample loaded on the ATR detector and then.

3.8 Nanoindentation

Nanoindentation tests were carried out on the surface modified pads using the NANOTEST 600[®] nanoindenter. The average pore size in the pads was approximately 350 microns. Therefore, a spherical stainless steel indenter with radius of curvature of 500 microns was chosen for nanoindentation which was expected not only to reveal the mechanical properties of the top surface of the pad but also to minimize the error due to the collapse of pores during measurement. Based on the results of preliminary indentation measurements on several PECVD treated pad specimens with varying coating time, the values for elastic moduli and hardness reported in this work use indentation data up to a depth of 1000 nm. While there is expected to be an effect of indentation depth due to coating time, selecting 1000 nm help compare data among a number of pad specimens with different coating time.

The effective modulus, E_{eff} , accounts for deformation of both the indenter and the specimen, can be expressed as^{65,66,67,68} :

$$\frac{1}{E_{eff}} = \frac{1-\nu_i^2}{E_i} + \frac{1-\nu_s^2}{E_s} \quad (2)$$

Where, E and ν are the elastic modulus and Poisson's ratio respectively; and subscripts s and i stand for the specimen and indenter respectively. Steel indenter is used in these studies. Values of Poisson's ratio and elastic modulus for steel indenter are 0.33 and 208 GPa, respectively. The value of Poisson's ratio for the pad was used as 0.3 as reported in the literature⁶⁹.

E_{eff} may be calculated⁶⁷ for a spherical indenter using the following relation:

$$E_{eff} = \frac{1}{2a} \frac{dP}{dh} \quad (3)$$

Where the terms P , a , and h are the penetration load, the radius of circle of contact at the maximum load, and the penetration depth, respectively. Using equation (3) and known values of ν_i , ν_s , and E_i , the value of the elastic modulus of the pad substrate can be estimated. Hardness (H) is determined by calculating the mean contact pressure^{3,66} at the maximum penetration load using the following relation:

$$H = \frac{P_{max}}{\pi a^2} \quad (4)$$

The estimated hardness and modulus of elasticity values reported in the present study were found to be reproducible and are mean value of a number of indentation experiments, to keep the uncertainty of measurement to minimum.

For studying the presence of different chemicals into the slurry dynamic polishing studies were carried out. These results are used as primary guidelines for following CMP studies. Static

dissolution studies are initially carried out to study the exact effect of each chemical on copper dissolution, while the electrochemical results gives ideas about exact chemical reactions due to different chemicals present in slurry. Chemical states of the copper surface due to reaction with the different chemicals into the solution are studied using XPS and SIMS analysis.

In the evaluation of pad surface modification, variation of the pad surface chemistry is extensively studied using the XPS analysis. Deconvolution of the individual XPS spectra's gives possible functional groups present on the pad surface. After dissociation of TEOS on the pad surface, variation in Si-OX (where X is C, H or N) moieties is extensively studies using FTIR analysis. The results obtained from XPS analysis are confirmed with the FTIR results. Variation of pad surface morphology due to deposition of TEOS is studied using SEM. Due to formation different species on the pad surface; variation pad's surface mechanical properties are studied using nana-indentation technique. Variation of these different species formation, proposed by XPS and FTIR results varies the pad's surface mechanical properties like elastic modulus and hardness. These mechanical properties are extensively studied and analyzed by the nonindentation studies.

CHAPTER 4. RESULTS AND DISCUSSION

4.1 Chemical Aspects

Numerous studies were performed to understand the CMP process in the Cu. For the development of slurry, water-Cu, Pourbaix diagram⁷⁰ (pH diagram) is widely used as one of the guidelines. Cu-H₂O potential pH diagram is shown in figure 5, the pourbaix diagram stability regions of Cu metal, Cu²⁺ ions, Cu⁺ oxide and Cu²⁺ oxides are located. From the pH diagram as proposed earlier^{3,5,27} one of the following two approaches have been adopted:

1. Use of Alkaline pH: From pourbaix diagram it can be interpreted that formation of oxide on the Cu surface take place and oxide layer is easily removed using mechanical action.
2. Use of Acidic pH: These acidic slurries enhanced the dissolution of Cu. However use of these slurries needs inclusion of some other chemicals in the slurry to inhibit the dissolution in concave areas.

Steigrwald *et al.* proposed that the removal of Cu could be achieved as a result of mechanical abrasion, and the role of chemical element was only to dissolve the abraded Cu particles rather than to etch the material directly from the surface. The complete and fast dissolution of the abraded particles in the CMP solution was very important in order to achieve defect free global planarity as point out by Kauffman *et al.* In active dissolution of the abraded particles both oxidants and complexing agents play a key role in the CMP process.

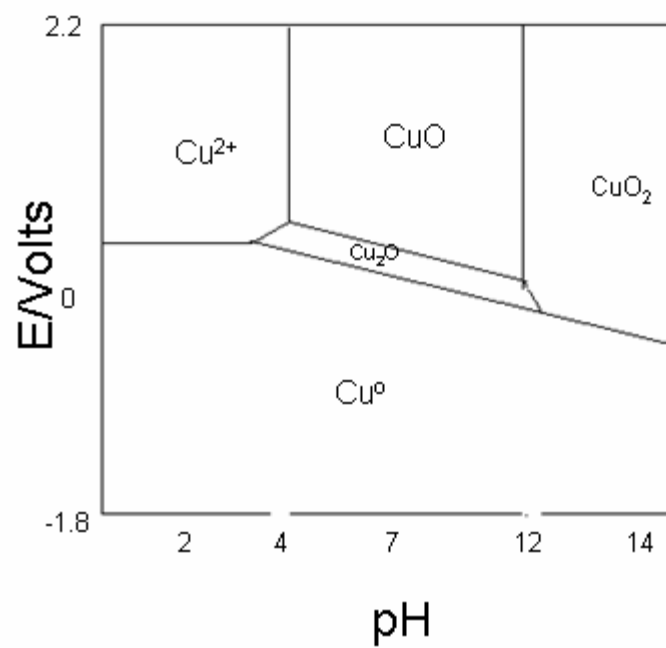


Figure 5. Cu-H₂O Pourbaix diagram.

Hydrogen peroxide is widely used oxidizing agent in Cu CMP industry. Powerful oxidizing agent, virtually can be used at any pH values, and clean oxidizer⁷¹ (clean oxidizer means it does not leave any byproducts which can further react with the Cu surface) is some of the key aspect of hydrogen peroxide which makes it popular in the CMP industry. Hydrogen peroxide is one of the most unstable compounds and it decomposes spontaneously as



Hirabayashi *et al.*⁷² proposed that the formation of an oxide film by H_2O_2 protects the recess region of Cu. On the protruded region, the removal of Cu took place both by mechanical abrasion and subsequent dissolution due to the formation of water-soluble Cu^{2+} -glycine chelate in the presence of glycine and H_2O_2 . However, the study¹⁶ neither addressed the Cu^{2+} -glycine- H_2O_2 interaction nor clarified the role of hydroxyl radicals on Cu removal. Hariharaputhiran *et al.*^{32,73} reported that the presence of H_2O_2 along with amino acid catalytically produced hydroxyl radicals, which attributed to the very high Cu-polishing rate. The Cu polish rate was found to increase with increase in glycine concentration. On the other hand, increase of H_2O_2 concentration resulted in a decrease in the polishing rate of Cu. Zhang *et al.*⁷⁴ have shown based on modeling study on Cu CMP that the removal rates of Cu increased with the increase of glycine concentration in the presence of 5 weight per cent of H_2O_2 . Various experiments have been carried out to understand the effect of each chemical is described in following sections:

4.1.1 Dynamic Polishing Studies

Initially some Dynamic polishing studies had carried out to determine fundamental direction of this study. Figure 6 shows the dynamic polishing of the Cu wafer at different pH

values. It can be observed from the figure that maximum dissolution rate obtained at pH value equal to 2. Hence most of the research work is done in acidic media at pH 2.

For the selection of inhibitors, initially C-600Y (Cabot Microelectronics Inc., Aurora, IL) slurry with presence of hydrogen peroxide and various chemicals are tested. Figure 7 shows the dynamic polishing result. Benzotriazole shows highest efficiency as a Cu corrosion inhibitor as compared to the other chemicals. The exact reaction of the BTA with the Cu has been described in the subsequent sections.

4.1.2 Dissolution Characteristics

4.1.2.1 Effect of Hydrogen Peroxide concentration variation

Figures 8(a) and 8(b) show the static removal rate of Cu as a function of hydrogen peroxide content with 0.1M glycine in pH 2 and pH 4 solutions, respectively. The dissolution rate of Cu was found to increase initially with an increase in H₂O₂ content in pH 2 up to about 5% and finally it decreased. The suppression of the dissolution rate with hydrogen peroxide content beyond 5% was probably attributed to the surface repassivation process. Although the presence of hydrogen peroxide initially enhances the polishing rate, other studies^{25,29,33} revealed a suppression of polishing rate at high concentration of H₂O₂ in the polishing slurry. It should be noted that the highest dynamic polishing rate of Cu was observed in pH 4 solution containing 2.5% of H₂O₂ with 0.1M glycine. Figure 8 (b) shows that the maximum Cu dissolution took place in pH 4 solution with 0.1 M glycine at 2.5% H₂O₂ and then start dropping down as further concentration increases.

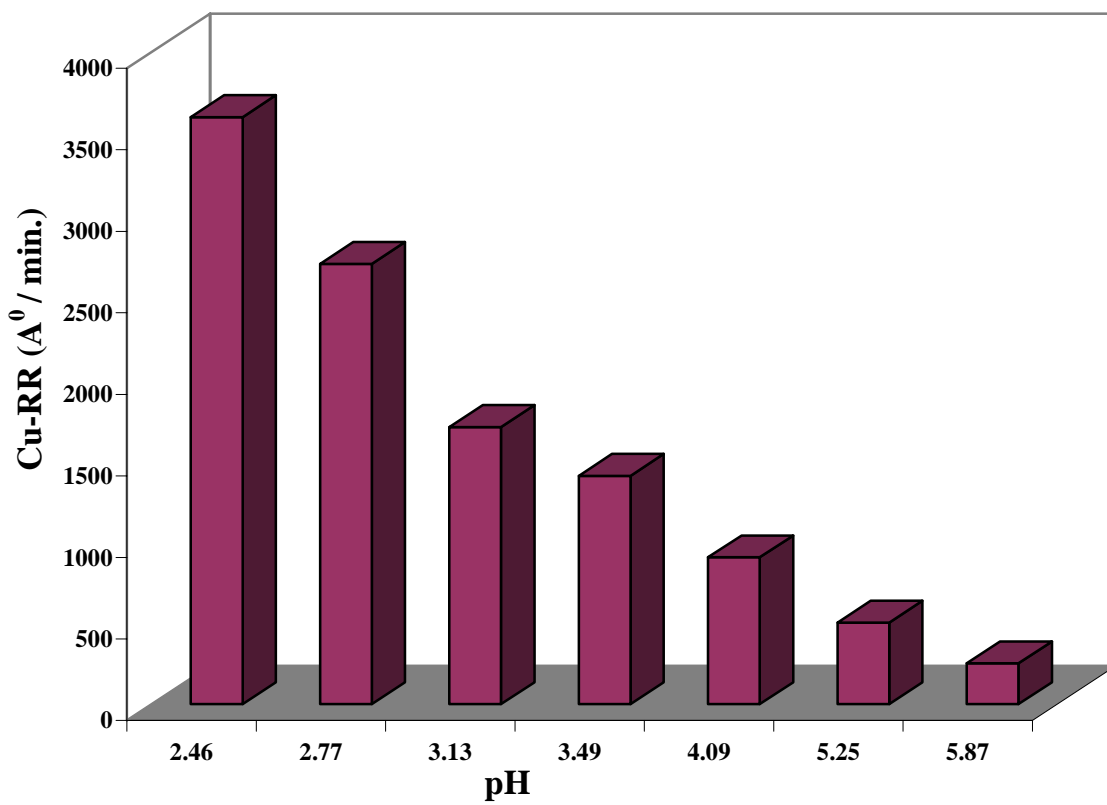


Figure 6. Dynamic polishing on Cu wafer at various pH values.

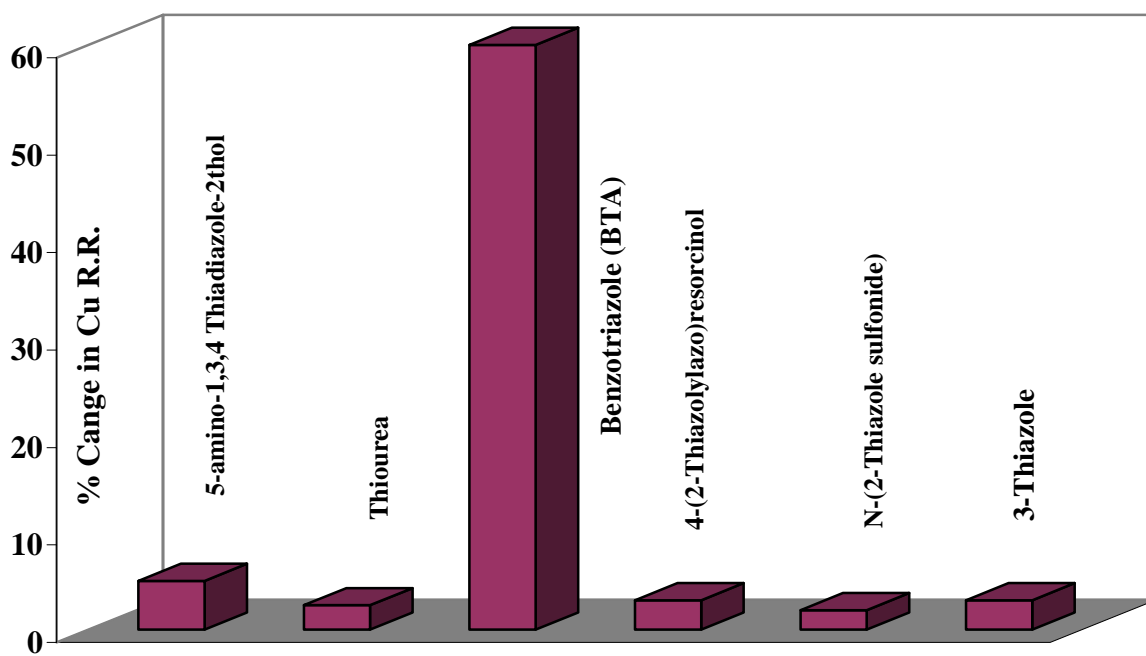


Figure 7. Comparison of various inhibitor efficiencies using dynamic polishing Studies.

Cu dissolution rate increases with increasing peroxide concentration. At some point, the dissolution rate is high enough to cause the surface concentration of Cu ions to reach solubility limit of Cu_2O at that particular pH value. Once this limit is reached, the oxide precipitates and suppressed the further dissolution of Cu. Hydrogen peroxide assisted in the formation of Cu-oxide, which subsequently formed the Cu^{2+} -glycine complex in the solution containing 0.1M glycine at pH 4. The trend of results in the present situation hints that the similar mechanism of Cu oxidation and subsequent complexation with glycine operates in solution at pH 2 with glycine and hydrogen peroxide.

4.1.2.2 Effect of pH variation on Cu dissolution

In the present investigation with 0.1M glycine and hydrogen peroxide in pH 2 solution, the removal rate was higher than that at pH 4 solution with similar concentration of glycine and H_2O_2 . Such higher dissolution rate at pH 2 was possibly due to the active dissolution of Cu at a faster rate as per the normal dissolution trend of metallic system at reduced pH. As such oxides of Cu are not stable^{5,42} at low pH level. At lower pH, the dissolution of Cu is balanced electrochemically by the reduction of oxygen. Another important observation in the present study is that the dissolution rate of Cu in pH 2 and pH 4 solution without hydrogen peroxide and with 0.1M glycine was almost undetectable in the present measuring system. Such results strongly indicate that glycine acted as a corrosion inhibitor in the absence of the oxidizing agent, as reported by others^{75,76}.

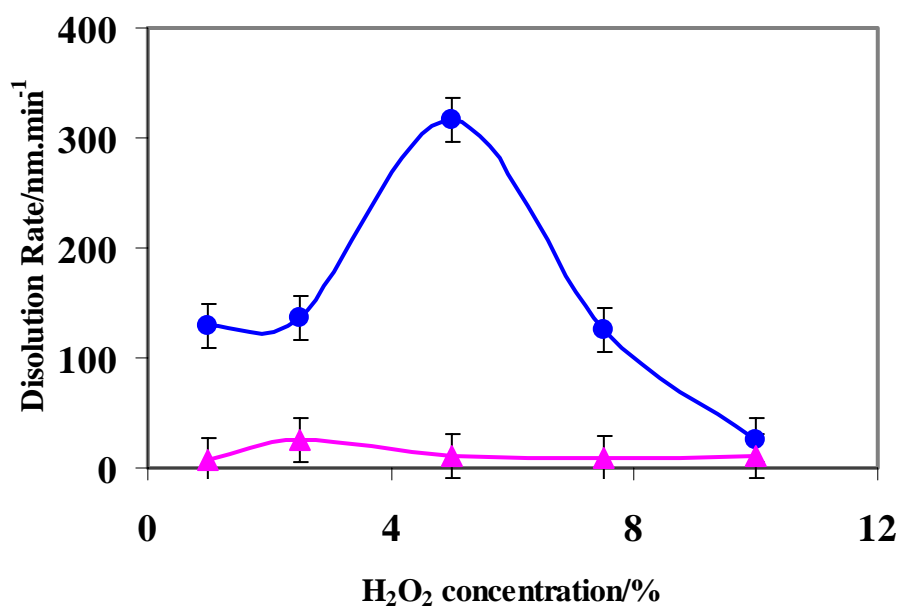


Figure 8. Effect of H₂O₂ content on the dissolution rate of Cu in solution containing 0.1M glycine at (a) pH 2, and (b) pH 4.

4.1.2.3 Effect of Glycine concentration variation

The effect of glycine concentration in the range of 0.01 to 1.0 M in solutions with 5% H₂O₂ at pH 2, 2.5% H₂O₂ at pH 2, and 2.5% H₂O₂ at pH 4 on the dissolution rate of Cu is presented on Figures 9(a), 9(b), and 9(c), respectively, which revealed that the maximum dissolution rate was observed at 0.1M glycine under all experimental conditions. Figure 2 also confirmed that the glycine did not inhibit the corrosion in the presence of hydrogen peroxide; rather it enhanced the dissolution process further.

4.1.2.4 Effect of Addition of BTA

Figure 10 depicts the effect of the concentration of benzotriazole (BTA) as inhibitor in pH2 solution along with 2.5 and 5% of H₂O₂ and 0.1M glycine. It can be observed in Figure 10 that the BTA decreased the dissolution rate. The reduction in the dissolution rate was more effective in the solution containing 5% H₂O₂. Such trend of results indicates that the BTA not only acted as corrosion inhibitor on Cu in the present solution but also interacts with the hydrogen peroxide. The inhibition efficiency was enhanced in the presence of high concentration of hydrogen peroxide. The enhancement of the inhibition efficiency in the present situation was possibly due to the formation of the Cu-BTA complex after reaction with the Cu-oxide. Growth of the Cu-BTA film occurs by ionic migration similar to that described in the formation of surface oxides. Besides, Cu-BTA film also takes part in polymerization process and eventually it acts as a diffusion barrier^{41,42}. Consequently, the corrosion of Cu was inhibited by the presence of BTA. Steigerwald *et al.* reported that the thickness of Cu-BTA film was almost 20 nm after 10 minutes of immersion in solution at pH 2.

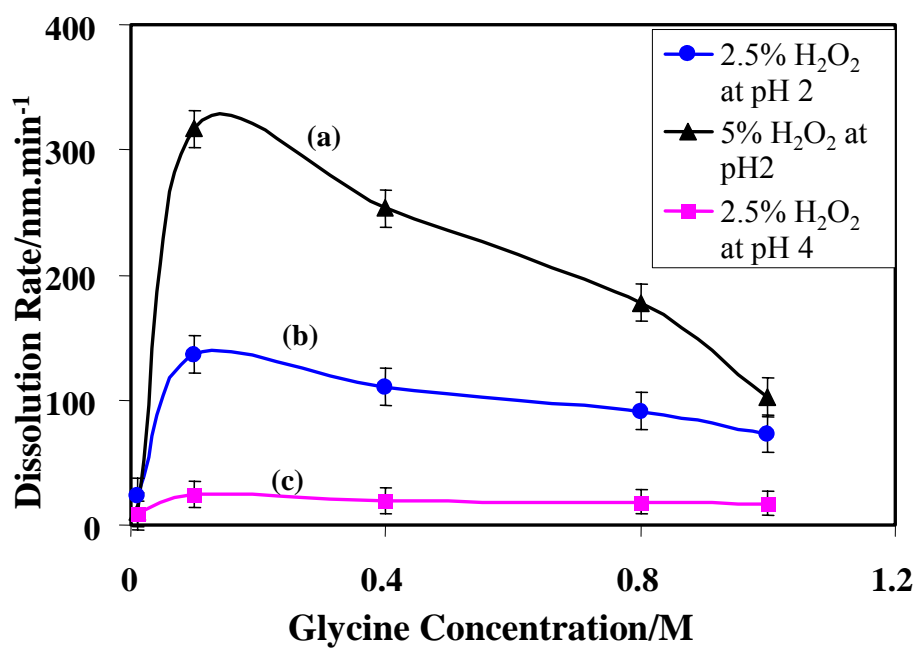


Figure 9. Effect of glycine content on the dissolution rate of Cu in solution (a) 5% H₂O₂ at pH 2, (b) 2.5% H₂O₂ at pH 2, and (c) 2.5% H₂O₂ at pH 4.

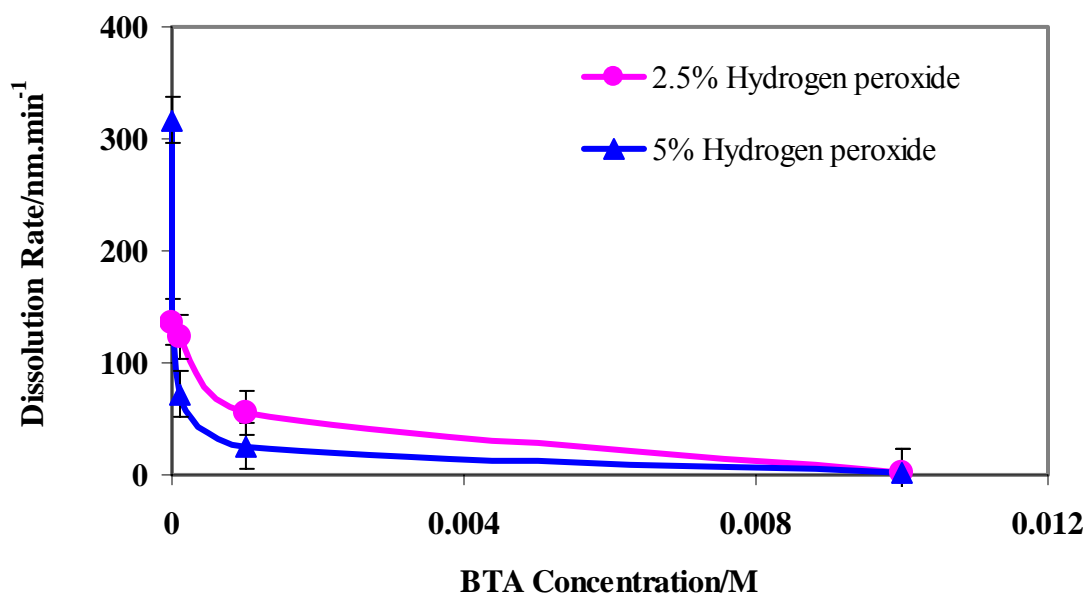


Figure 10. Effect of benzotriazole content on the dissolution rate of copper in solution containing 0.1M glycine at pH 2 with 2.5% and 5 % H₂O₂.

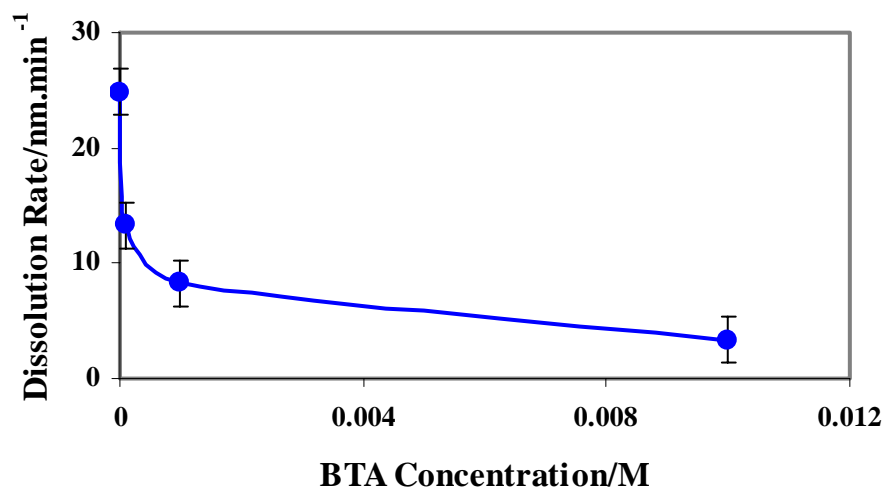


Figure 11. Effect of benzotriazole content on the dissolution rate of copper in solution at pH 4 containing 2.5% H₂O₂ and 0.1M glycine.

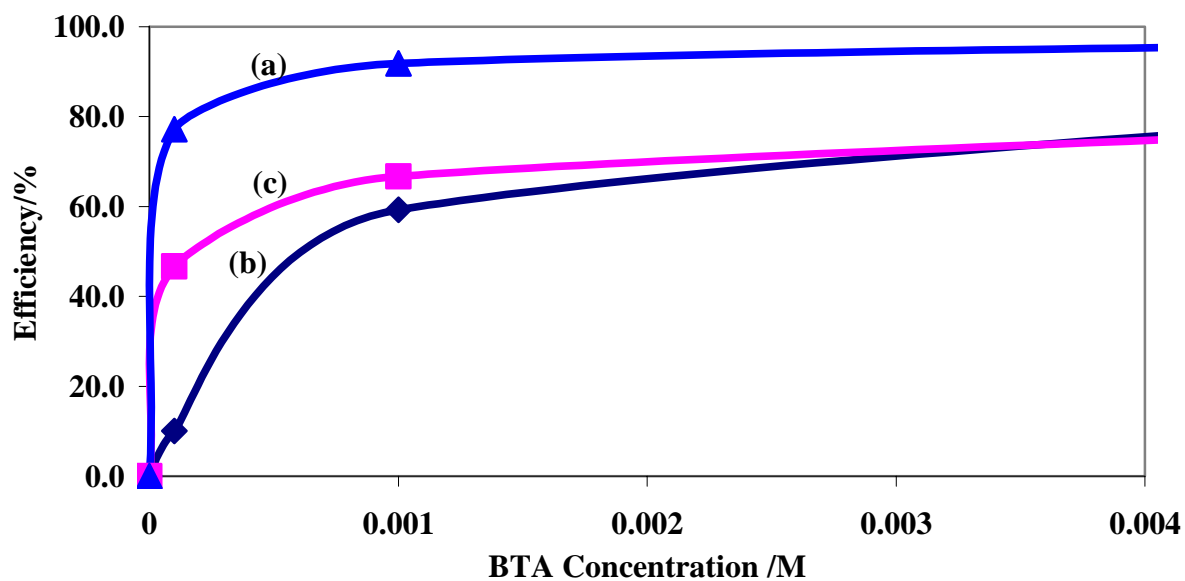


Figure 12. Effect of pH and H₂O₂ content on the inhibition efficiency of benzotriazole (BTA) on copper dissolution in solution containing 0.1M glycine (a) 5% H₂O₂ at pH 2, (b) 2.5% H₂O₂ at pH 2, and (c) 2.5% H₂O₂ at pH 4.

The effect of benzotriazole in pH 4 in the presence of 2.5% of H₂O₂ and 0.1M glycine can be observed from the Figure 11. It follows the similar trend as that observed for pH 2 solution with 2.5 % of H₂O₂ and 0.1 M glycine.

The inhibition efficiency (η) values were estimated from the dissolution rate data as a function of BTA with respect to the dissolution rate in similar solution composition in absence of BTA as per the following relation:

$$\eta = \left(1 - \frac{k_d}{k_d^0} \right) 100 \quad (6)$$

Where, k_d and k_d^0 are the dissolution rate of copper in a solution with BTA and without the presence of BTA, respectively. Estimated η values as a function of BTA concentration on Cu in solutions containing 0.1M glycine with 5% H₂O₂ at pH 2, 2.5% H₂O₂ at pH 2, and 5% H₂O₂ at pH 4 are presented in Figures 12(a), 12(b) and 12(c), respectively. The inhibition efficiency increased with the increase in BTA concentration, which further confirms the inhibition action of BTA. The effect of benzotriazole in pH 4 solution in the presence of 2.5% of H₂O₂ and 0.1M glycine can be observed from the Figure 12(c). It follows a similar trend as that observed for pH 2 solution with 2.5 % of H₂O₂ and 0.1 M glycine. Studies from Luo *et al.* shows that BTA is a weak acid and dissociate according to the following:



Tommessani *et al.* mentioned that acidity largely weakens the protective action and persistence of the surface film.

4.1.2.5 Effect of pH: on Cu –BTA complex formation

The effect of pH on the nucleation could be explained by looking at the reaction taking place at the metal surface.



The reaction takes place with Cu^+ or one of its complexes depending on the concentration of anion into the solution. At low pH, the concentration of BTA^- is expected to be less according to the equation (8) which would definitely reduce the rate of Cu-BTA film formation, ultimately a reduced value of inhibition efficiency. The inhibition efficiency values of BTA at 0.01M concentration level in solutions containing 0.1M glycine and 2.5% H_2O_2 at pH 2 and at pH 4 were found to be 10 and 47 %, respectively. The trend of the pH dependence of inhibition efficiency was found to be similar at higher concentration of BTA, which confirms the dissociation as per equation (8) and subsequent formation of Cu-BTA complex.

Increasing concentration BTA to certain extend will increase the reaction rate which ultimate result in faster nucleation rate resulting in the faster Cu(I)BTA film formation. At the lower value of pH the BTA is protonated and as the pH value increases protonated BTA concentration decreases which causes faster reaction, one of the main reason for improved inhibition efficiency of BTA with increasing pH values.

Figure 12 also ascertained that the effectiveness of BTA as a corrosion inhibitor was enhanced due to the presence of H_2O_2 ; otherwise it would have been impossible to get the corrosion inhibition effect at such a low level BTA concentration of 0.01M. Furthermore, the efficiency values in solutions at pH 2 with 0.01M BTA and 0.1M glycine at 2.5% and at 5% H_2O_2 were 10, and 77%, respectively. The presence of hydrogen peroxide has enhanced the

formation of Cu-BTA complex. As usual, the inhibition action was found to saturate at about 0.01M concentration of BTA.

4.1.3 Electrochemical Polarization Behavior

Potentiodynamic polarization tests were carried out to study the passivation and dissolution behavior of Cu. Potentiodynamic polarization provides information in wide range as compared to Tafel plots⁷⁷; it also gives additional information about corrosion kinetics and localized corrosion. I_{corr} and E_{corr} values measured from polarization curves.

Polarization plots for Cu in solutions at pH 2, pH 2 with 0.1M glycine are shown in Figures 13(a), and 13(b), respectively. Figures 13(c), 13(d), 13(e) and 13(f) present the polarization plots of Cu in solution at pH 2 with 0.1M glycine containing 2.5% H_2O_2 , 5% H_2O_2 , 7.5% H_2O_2 , and 10% H_2O_2 , respectively. Some loops and kinks are observed in the passive region which suggests the possibility of pitting corrosion on the Cu samples. This may be attributable to the sample preparation techniques used.

Micro pits on the sample surface probably provide sites for the observed pitting corrosion. Figures 14(a), 14(b) and 14(c) present the polarization plots for Cu in pH 2 solution containing 0.1M glycine without H_2O_2 , with 5% H_2O_2 , and with 5% H_2O_2 along with 0.01M BTA, respectively. The values of E_{corr} , I_{corr} , and the polarization resistance (R_p) were estimated from the polarization studies on Cu in various solutions which are shown in Table 2. The value of the open circuit potential (OCP) in pH 2 solution without any additive was found to be 151 mV versus Ag/AgCl reference electrode and which drops to -30 mV with the addition of 0.1M glycine.

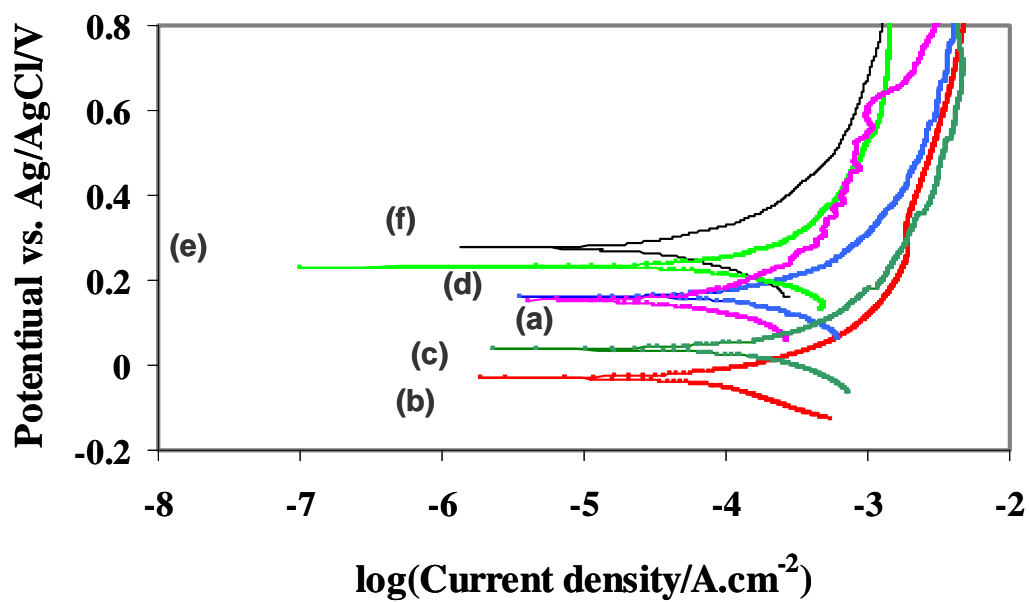


Figure 13. Potentiodynamic polarization plots of copper in solution at (a) pH 2; (b) pH 2 with 0.1M glycine; and pH 2 with 0.1M glycine and H₂O₂ content of (c) 2.5%, (d) 5%, (e) 7.5%, and (f) 10%.

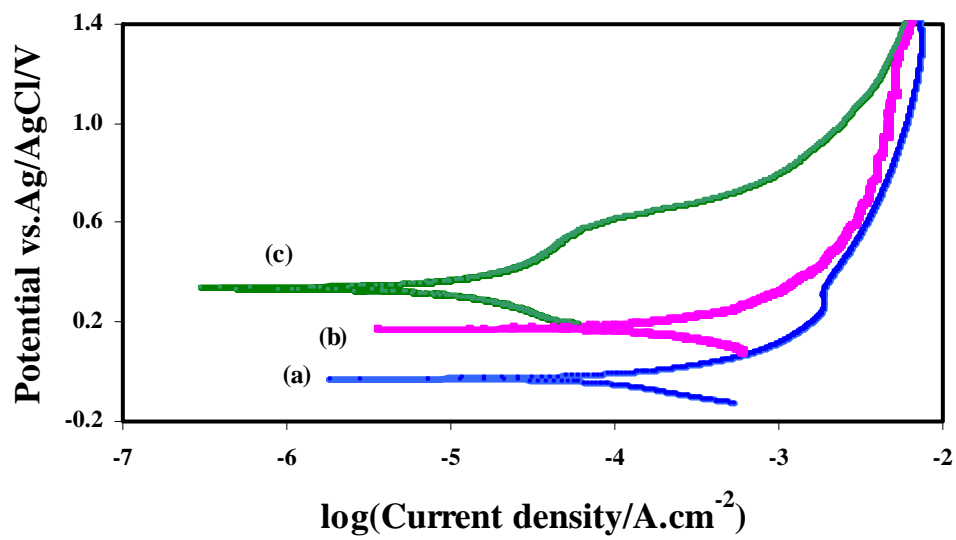


Figure 14. Potentiodynamic polarization plots of copper in solution at pH 2 with 0.1M glycine (a) without H₂O₂ , (b) 5% H₂O₂, and (c) 5% H₂O₂ with 0.01M BTA.

Figure 6 also indicates a gradual increase in open circuit potential value with increased H_2O_2 concentration. Such upward shift of the polarization diagram was probably due to the formation of a thin oxide layer on the Cu surface due to the presence of the oxidizer. Such trend was also observed in the earlier CMP study²⁵ in solutions containing 0.1M glycine at pH 4. Such oxide film possibly provided an increased barrier to the transport of ionic and electronic species leading to an upward shift in the polarogram. The corrosion current density (I_{Corr}) value was initially increased with hydrogen peroxide content, attained a plateau, and then found to decrease with time. Similar behavior was also observed during the dissolution rate studies (Figure 8) as a function of H_2O_2 content in pH 2 solution with 0.1M glycine.

The values of corrosion current density were found to be the highest in the solution at pH 2 with 0.1M glycine and 5% H_2O_2 . The dissolution rate of Cu was also found to be the highest in solution with such composition. The trend of I_{corr} values correlates with the outcome of the dissolution rate measurements in corresponding solution composition in the present study. The corrosion current density with 0.1M glycine at pH 2 was observed to be higher than that of pH 2 buffer solution as shown in Table 2. The exact cause for such result, however, is unclear at this time. Furthermore, dissolution rate of Cu in pH 2 solution with 0.1M glycine was too low to be measured. The polarization resistance was estimated from the slope of the linear portion of the plot of overpotential from the OCP vs. current density in all the cases. The value of R_p was found to be the lowest at pH 2 solution in presence of 0.1M glycine and 5% H_2O_2 . The estimated values of the polarization resistance were found to be inversely proportional to the value of corrosion current density. The R_p value was found to be the highest in the case of Cu immersed in pH 2 solution with 0.1M glycine, 5% H_2O_2 and 0.01M BTA. The corrosion current density was observed to be the lowest under such condition, indicating the inhibiting effect of benzotriazole

on Cu in aggressive corrosion condition. Such trend corroborates the findings of the dissolution rate measurement in the present investigation (Figure 10).

4.1.4 X-ray Photoelectron Spectroscopy (XPS) analysis of Cu surface

XPS studies were carried out to understand the interaction of H_2O_2 , glycine and BTA on Cu surface. Peak-fitted Cu(2p) XPS spectra taken from the surface of Cu after immersing for 10 minutes in solutions at pH 2 containing 5% H_2O_2 , 5% H_2O_2 with 0.1M glycine, and 5% H_2O_2 with 0.1M glycine and 0.01M BTA, are shown in Figures 15(a), 15(b), and 15(c), respectively. The Cu ($2p_{3/2}$) and Cu ($2p_{1/2}$) peaks are found to be separated by a binding energy value of 19.9 eV which is identical with the value reported in the literature⁷⁸. Figure 15(a) reveals Cu ($2p_{3/2}$) peaks at the binding energy values of 932.5 and 933.6 eV which are due to metallic Cu (Cu^0) and CuO, respectively. The formation of native oxide on the surface was due to the reaction of H_2O_2 on the Cu surface. The Cu (2p) envelope in Figure 15(a) also shows the satellite peak which further confirms the formation of bivalent copper oxide on the surface^{25,78}.

Table 2. E_{corr} , I_{corr} , and the polarization resistance (R_p) estimated from the polarization studies on copper in various solutions.

Addition of different chemicals in pH 2 solution.	Electrochemical Polarization Parameters		
	$E_{\text{Corr}}/\text{mV}$ Ag/AgCl	I_{Corr} $\mu\text{A. cm}^{-2}$	R_p Ohm. cm^{-2}
none	151	158	268
0.1M glycine	-30	393	213
0.1M glycine + 2.5% H_2O_2	38	141	124
0.1M glycine + 5% H_2O_2	173	616	92
0.1M glycine + 7.5% H_2O_2	232	266	121
0.1M glycine + 10% H_2O_2	277	142	489
0.1M Glycine+ 5% H_2O_2 + 0.01M BTA	336	8	2867(large)

After deconvoluting the Cu(2p) envelope that was obtained from the Cu specimen after exposing to pH 2 solution with 5% H₂O₂ and 0.1M glycine for 10 minutes, three peaks at 932.8, 933.8 and 935.5 eV were found as shown in Figure 15(b). The peaks at binding energy values of 932.8 and 933.8 eV confirmed the presence of metallic copper (Cu⁰) and CuO, respectively. The peak at 935.4 eV is attributed to Cu-glycine complex present on the surface. The low intensity of the Cu (2p_{3/2}) peak at 935.4 suggests that in the presence of glycine the oxide film get dissolved in the solution after forming a soluble complex. The high rate of removal in pH 2 with 5% H₂O₂ and 0.1M glycine solution is due to formation of Cu-glycine complex and its easy removal by subsequent dissolution. Similar results were obtained for the pH 4 solution in previous study. Figure 15(c) shows the deconvoluted Cu(2p) spectrum obtained from the surface of Cu after immersing for 10 minutes in a solution at pH 2 containing 5 % H₂O₂, 0.1M glycine and 0.01M BTA, which shows only one peak at 932.4 eV. The peak represents Cu-BTA complex on the surface of Cu. Similar binding energy value for the Cu-BTA complex was reported by others⁷⁹. It can be mentioned that the full-width-half-maxima value of the Cu (2p_{3/2}) envelope in Figure 15(c) was less than those in Figures 15(a) and 15(b). The full-width-half-maxima value of the Cu (2p_{3/2}) envelopes in Figure 15(a), 15(b), and 15(c) were found to be 3.2, 3.4 and 2.4 eV, respectively.

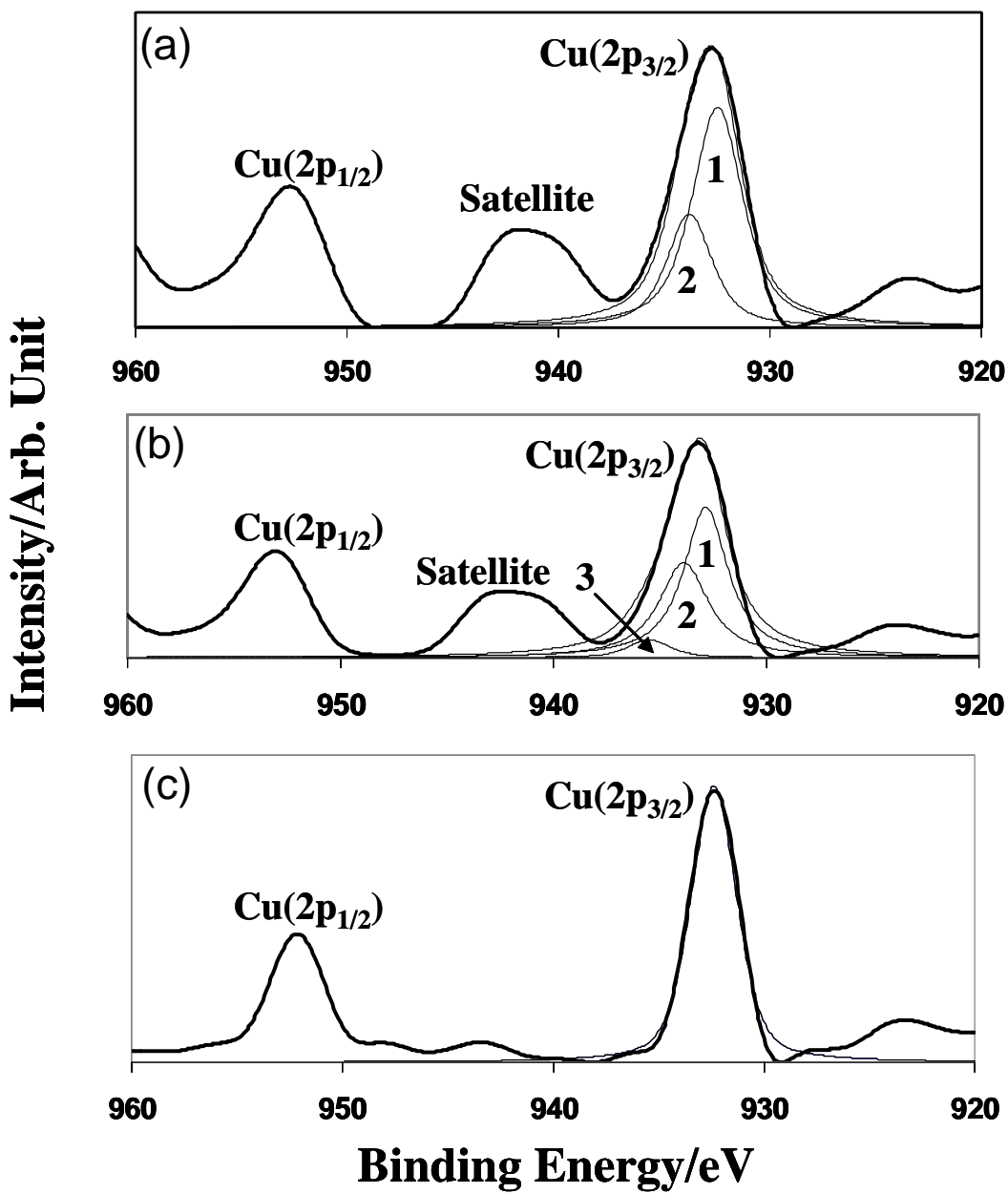


Figure 15. Peak-fitted Cu (2p) XPS spectra from surface of copper immersed for 10 minutes in solution at pH 2 (a) 5% H_2O_2 (b) 5% H_2O_2 with 0.1M glycine, and (c) 5% H_2O_2 , 0.1M glycine with 0.01M benzotriazole [1. Cu^0 , 2. CuO , 3. Cu-glycine complex, and 4. Cu-BTA complex].

Moreover, the satellite peak intensity was also at the bare minimum. Such XPS spectrum strongly indicates that the formation of Cu-oxide was absent in the presence of BTA. In highly acidic environment, BTA has tendency to form thick film on the Cu surface. To further confirm the formation of Cu-glycine and Cu-BTA complexes on the surface, the corresponding N (1s) XPS spectra were analyzed. The peak fitted XPS spectra of N (1s) that obtained from the Cu surface after 10 min treatment in solution at pH 2 containing 5% H₂O₂ and 0.1M glycine without and with 0.01M BTA are presented in Figures 16(a) and 16(b), respectively. The N (1s) peak for Cu-glycine complex in Figure 16(a) was observed at 399.6 eV, which matches well with the values in the literature^{25,622}. The N (1s) peak corresponding to Cu-BTA complex was reported²⁹ to be at 399.7± 0.2 eV. After peak fitting, a peak was observed in Figure 16(b) at a binding energy value of 399.8 eV, which was possibly attributed to Cu-BTA complex on the surface of Cu. There was no indication of Cu⁰, CuO or Cu₂O on the surface of the Cu specimen treated with 0.01M BTA in Figure 15(c). The Cu-BTA complex was possibly polymerized and the thickness must have been more than 50 nm, so that the XPS signal from the Cu substrate underlying the Cu-BTA film was not detected. Similar trend of XPS results was observed for the Cu specimen immersed in various solutions containing 0.1M glycine and 2.5% H₂O₂ without and with 0.01M BTA at pH 4.

Results of the dissolution study and electrochemical measurements indicate that the Cu dissolves at a very rapid rate in pH 2 solution with 5% H₂O₂ and 0.1M glycine, while XPS investigation revealed the formation of Cu-glycine complex on the surface of Cu. Extensive electrochemical studies by Aksu and Doyle⁸⁰ on glycine in aqueous solution shows that glycine can exist in aqueous solutions in three different forms namely cation (⁺H₃NCH₂COOH), Zwitterions (⁺H₃NCH₂COO⁻), and anion (H₃NCH₂COO⁻). The equilibrium concentrations of

these species depend on the pH of the solution as also observed by others^{31,32}. In absence of other organic or inorganic species, the cations and anions predominate at pH values below 2.35 and above 9.778, respectively.

The zwitterions predominate at pH values intermediate between 2.35 and 9.78. Glycine forms soluble complexes with both cupric and cuprous ions. While the principal Cu-glycine complexes for cupric are $\text{Cu}(\text{H}_3\text{NCH}_2\text{COO})^{2+}$, $\text{Cu}(\text{H}_2\text{NCH}_2\text{COO})^+$, and $\text{Cu}(\text{H}_2\text{NCH}_2\text{COO})_2$, and for the cuprous is $\text{Cu}(\text{H}_2\text{NCH}_2\text{COO})_2^-$.

4.1.5 Secondary Ion Mass Spectroscopy Analysis

Secondary Ion Mass spectroscopy (SIMS) has the ability to deliver useful information in complex adsorption systems⁸¹. High sensitivity, surface specificity, polyatomic adsorbents, molecular information, hydrogen detection and isotopic discrimination are some of the attractive advantages of the SIMS technique. SIMS depth profiling have detection limit in ppm range⁸¹.

In order to investigate the type of Cu-glycine complex formed during immersion of Cu in solution at pH 2 with 5% H₂O₂ and 0.1M glycine, SIMS analysis was carried out. The SIMS depth profiles on Silica (SiO₂) wafer, having 1 micron thick Cu layer treated with 2.5% Hydrogen peroxide and pH 4 solution with and without glycine have been shown in figure 17(a) and Figure 17 (b) respectively. It can be observed from figure 17 (a) that Cu and silicon oxide interface is occurred after depth profiling of around 1500seconds. As mentioned in earlier sections hydrogen peroxide in acidic solutions dissociates and perhydroxyl ion is formed. These ions are stable in acidic solution and passivate the Cu surface. An oxide film is formed on the Cu surface. Oxide film formed on the Cu surface protects the dissolution of Cu. XPS results confirm the formation of the oxide layer on the Cu surface. Cu and SiO₂ interface occurred after around 750 seconds of depth profiling time for the sample treated with pH 4 and 2.5 % hydrogen peroxide with 0.1M glycine. Reduction in the depth profiling time is due to active dissolution of Cu in the solution. To study the Cu-glycine formation SIMS depth profile analysis on Cu sample is carried out. Cu sample treated with the pH 2 solution and 5% hydrogen peroxide and glycine is shown in figure 18.

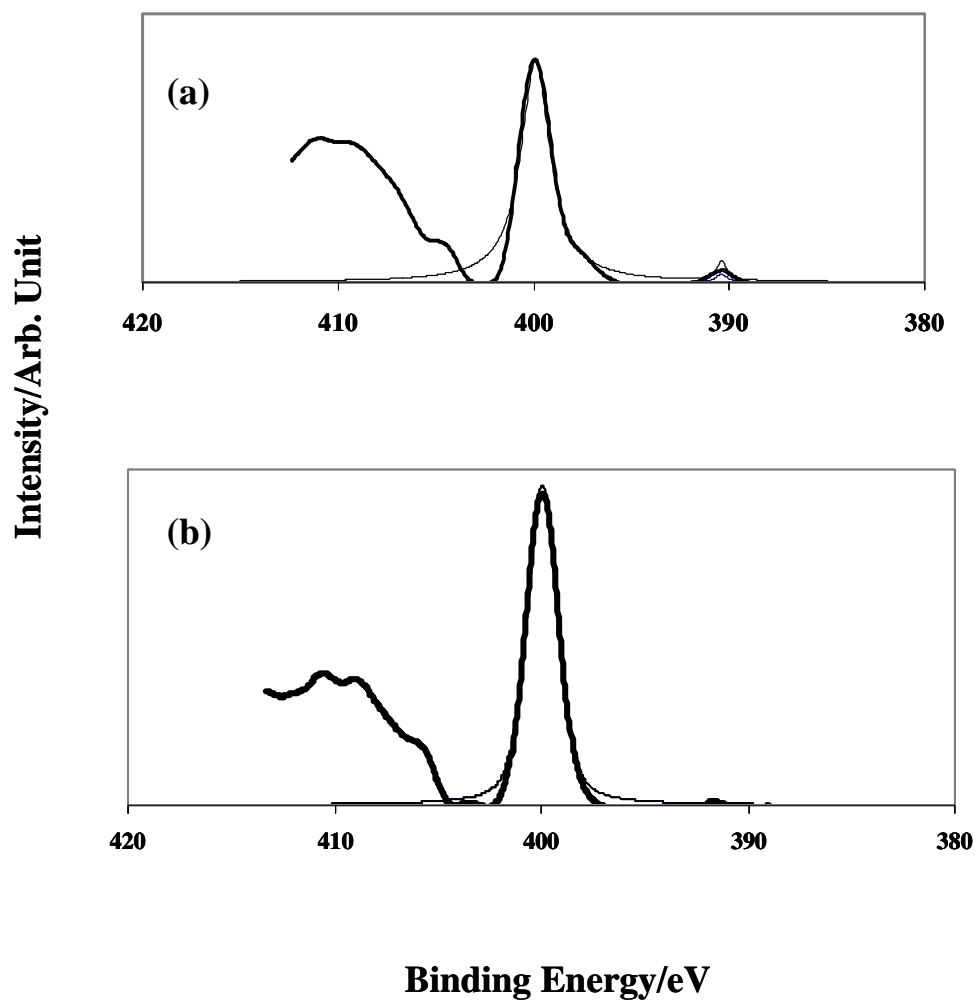


Figure 16. Peak-fitted XPS N(1s) spectra from surface of copper immersed for 10 minutes in solution at pH 2 containing 5% H₂O₂ and 0.01M glycine (a) without benzotriazole, and (b) with 0.01M benzotriazole.

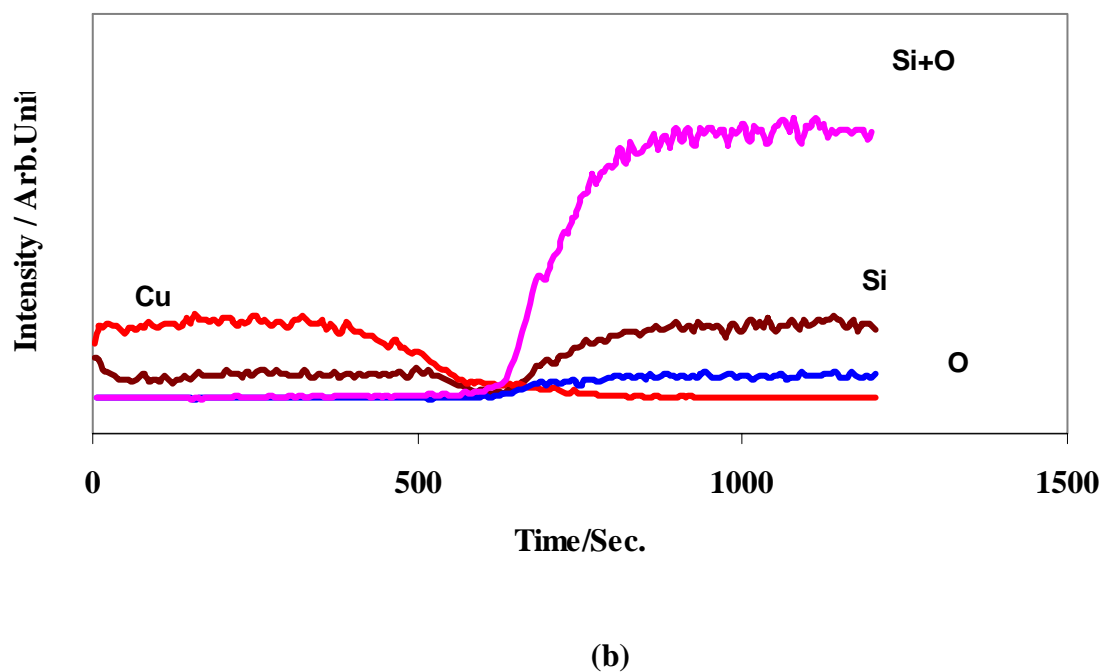
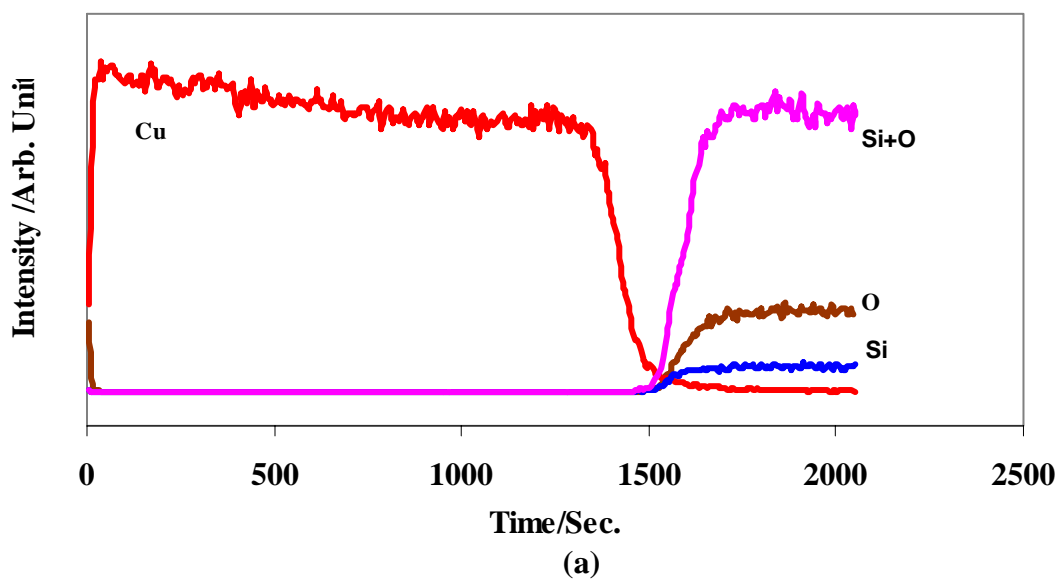


Figure 17. SIMS depth Profile of Cu-wafer after immersing in solutions at pH 4 for 15 min containing (a) 2.5% H₂O₂, and (b) 2.5% H₂O₂ and 0.1M Glycine.

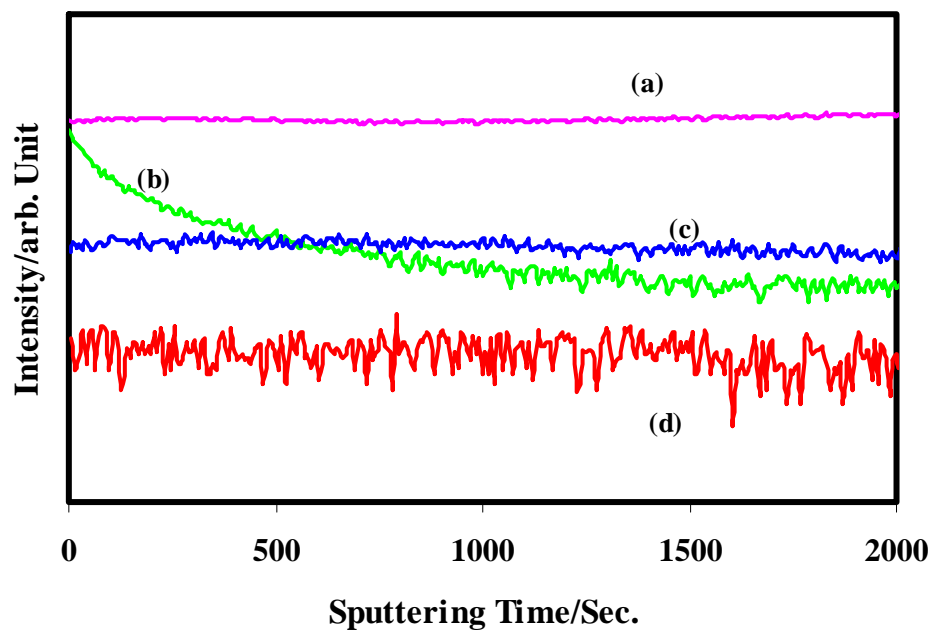


Figure 18. SIMS depth profile on the copper surface after treating with pH 2 solution with 0.1M glycine and 5% H₂O₂ (a) Cu, (b) -NH₂CH₂, (c) Glycine, and (d) Cu(H₂NCH₂ COO)⁺

Figure 18 depicts the concentration profiles of Cu, $-\text{H}_2\text{NCH}_2$, glycine, and Cu-glycine $[\text{Cu}(\text{H}_2\text{NCH}_2\text{COO})^+]$ that are shown in Figures 18(a), 18(b), 18(c), and 18(d), respectively. These species have corresponding mass of 63, 30, 76, 137 Dalton, respectively. The species with atomic mass 30 and 76 were from the fragments of the glycine and glycine with hydrogen, respectively. These were found to be the characteristic species obtained in SIMS analysis of Cu surface treated with glycine solution. Although Cu-glycine complexes have high mass and therefore the yield of such species in SIMS analysis is low. Moreover, breaking up of such complex species during interaction with the ions in SIMS is highly likely. Nevertheless, the Cu-glycine species with mass 137 was detected in the depth profile [Figure 18(d)] which was formed in the solution containing 0.1M glycine and 5% H_2O_2 at pH 2. In the presence of hydrogen peroxide, Cu oxidizes to CuO which subsequently form the $[\text{Cu}(\text{H}_2\text{NCH}_2\text{COO})^+]$ complex. The formation of such highly soluble complex was responsible for rapid dissolution of Cu under such condition.

To study the detail fragmentation of glycine under the ions, negative TOF-SIMS spectra were obtained from Glycine powder is shown in figure 19(a). Dominant peaks were identified as $[\text{H}_2\text{N}-\text{CH}_2]$ (m/z : 30), $[\text{H}_2\text{N}-\text{CH}_2-\text{COOH} + \text{H}]$ ($m/z = 76$). These two peaks are characteristic peaks of the glycine. To confirm these results similar study has been done on deuteriated glycine powder. In this isotope of glycine, three hydrogen in glycine molecule is replaced by the protonated hydrogen.

Figure 19 (b) shows the negative TOF-SIMS spectra on D-Glycine powder. From the results dominant peaks are observed at 32 and 79 Dalton. These two peaks corresponds to the $[\text{D}_2\text{N}-\text{CH}_2]$ ($m/z = 32$), $[\text{D}_2\text{N}-\text{CH}_2-\text{COOD} + \text{H}]$ ($m/z = 79$) respectively. This result confirms earlier results that peak at 30 and 76 are characteristics of glycine.

The inhibiting effect of BTA is mostly due to the formation of a protective Cu-BTA-Cu polymeric film as reported by others^{82,83, 33,34}. As already mentioned in previous sections at lower pH, BTA predominantly presents as protonated species that reduce the chemisorptions on the Cu surface which is already positively charged, thereby, decreasing the inhibition efficiency of BTA in acidic solution. SIMS study by Notoya *et al.*⁸⁴ on the formation of various metal-BTA films including Cu showed that BTA exhibited the highest inhibition efficiency on Cu at pH 6. Ion fragments originating from BTA were all negative ions such as -CN^- , C_3N^- , $\text{C}_6\text{H}_4\text{N}^-$, $\text{C}_6\text{H}_4\text{N}_3^-$, $[\text{Cu}(\text{C}_6\text{H}_4\text{N}_3)_2]^-$ having mass of 26, 50, 90, 118, 299 amu, respectively.

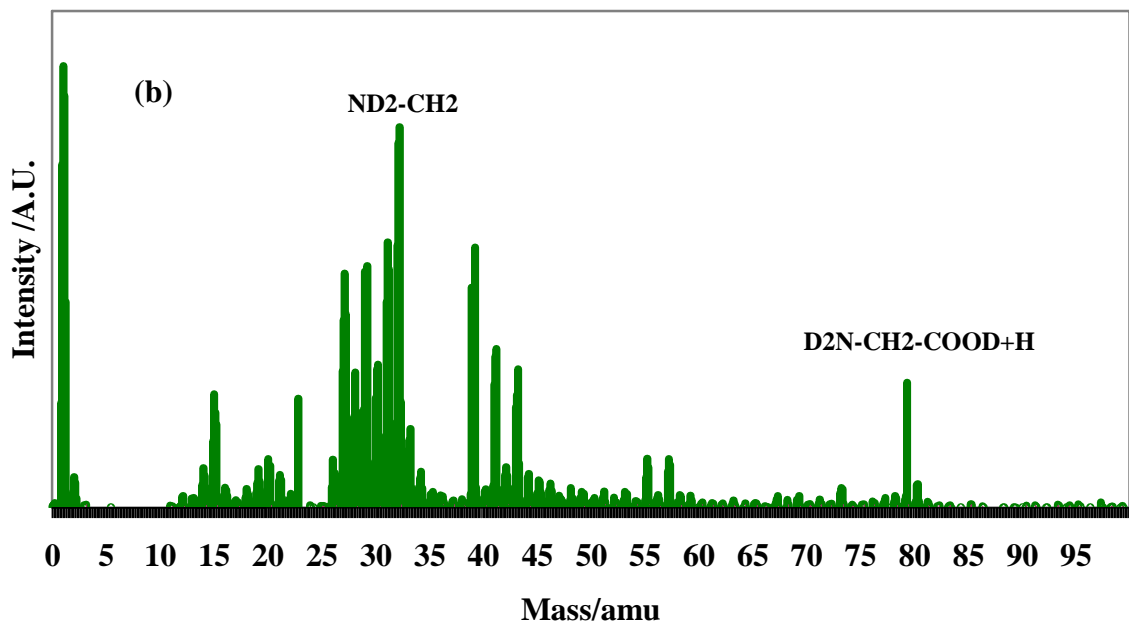
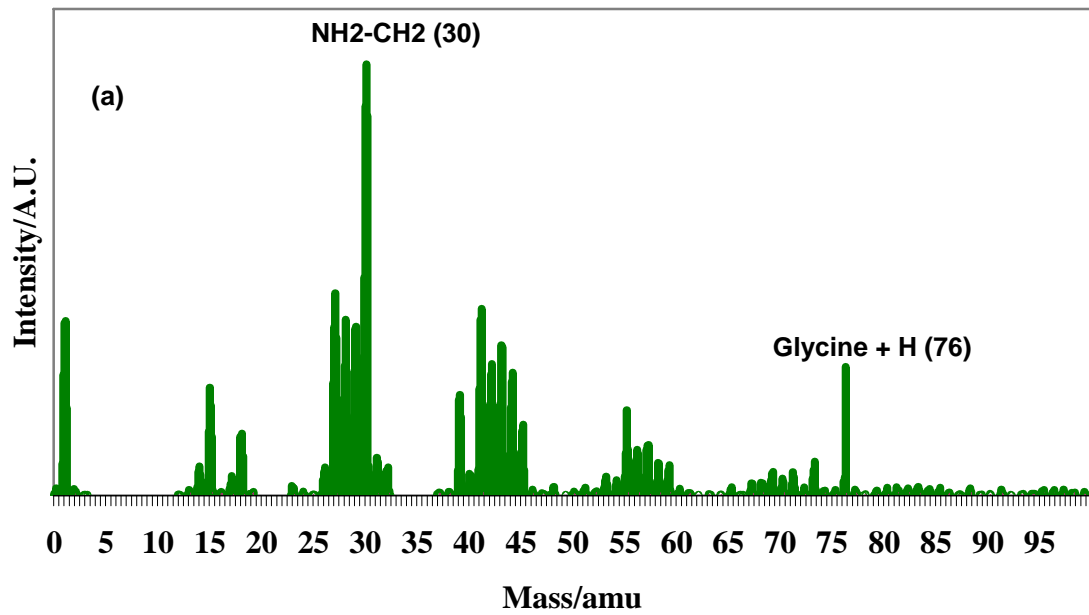


Figure 19. TOF-SIMS spectra on (a) glycine; (b) D-glycine powder.

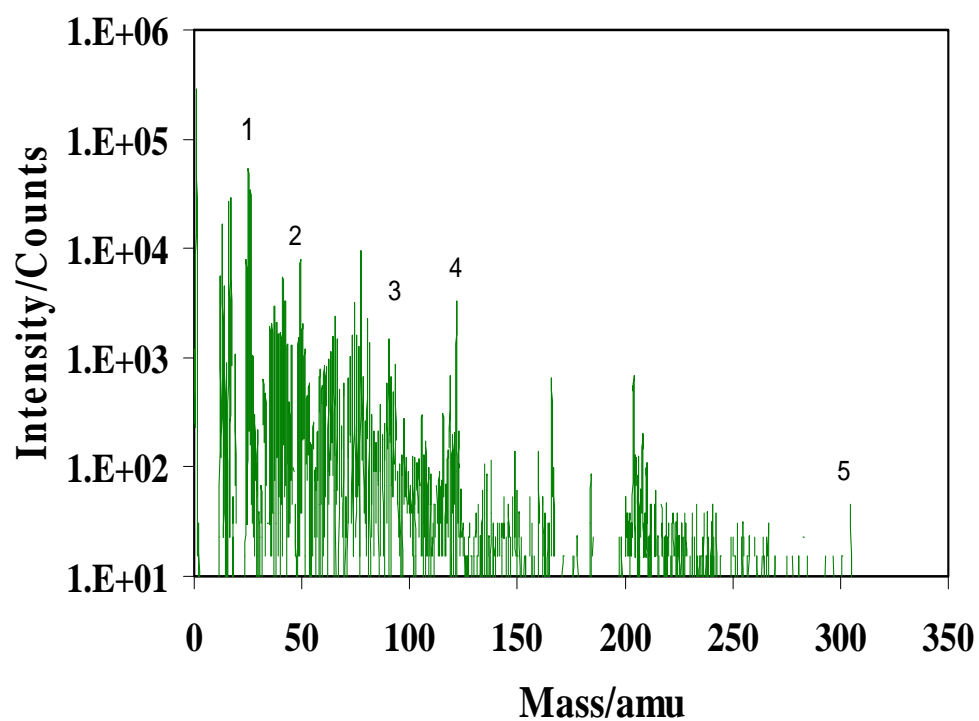


Figure 20. Static SIMS spectrum from the copper surface after treating in pH 2 solution with and 5% H_2O_2 , 0.1M glycine and 0.01M BTA. Peaks identified at 1. CN^- , 2. C_3N^- , 3. $\text{C}_6\text{H}_4\text{N}^-$ 4. $\text{C}_6\text{H}_4\text{N}_3^-$ 5. $[(\text{Cu}^+) (\text{C}_6\text{H}_4\text{N}_3^-)_2]$.

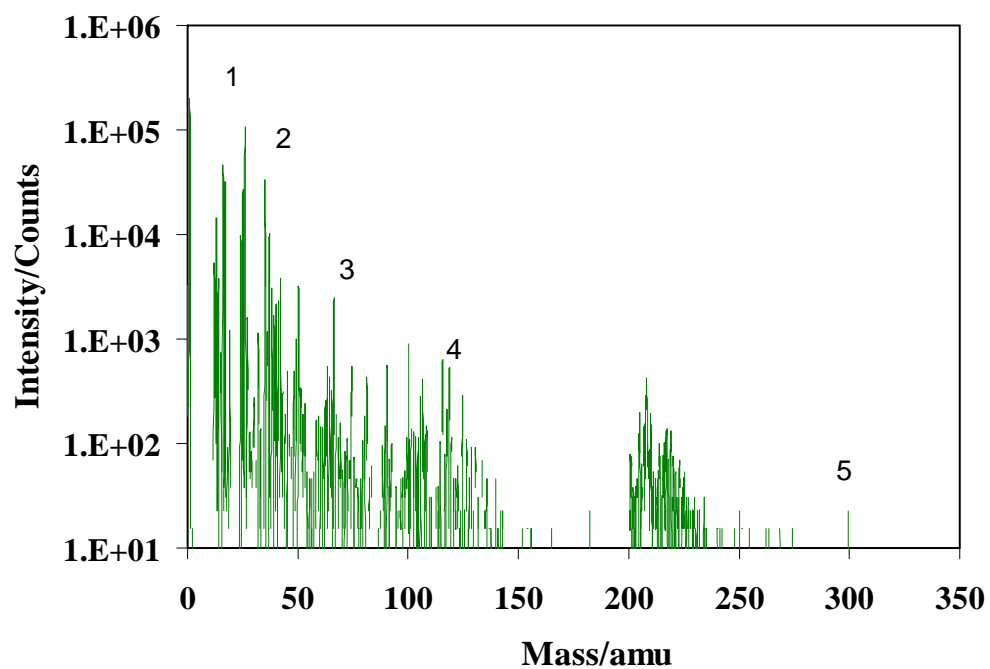


Figure 21. Static SIMS spectrum from the copper surface after treating in pH 4 solution with and 5% H_2O_2 , 0.1M glycine and 0.01M BTA. Peaks identified at 1.CN⁻, 2.C₃N⁻, 3.C₆H₄N⁻, 4.C₆H₄N₃⁻, 5.[(Cu⁺)(C₆H₄N₃⁻)₂].

Static SIMS spectra from the surface of Cu specimens treated with solutions containing 5% hydrogen peroxide, 0.01M glycine and 0.01M benzotriazole at pH 2 and pH 4 are presented in Figures 20, and 21, respectively. Figures 20 and 21 revealed the presence of all of the above mentioned peaks. Intensity of peaks observed in the solution at pH 4 is higher than that at pH 2. As per equation (7), the presence of BTA^- species in the solution at pH 4 is expected to be higher than that at pH 2. Therefore, the extent of Cu-BTA film formation was more in the solution at pH 4 compared to that at pH 2, which attributed to an increased intensity of SIMS signal from the Cu specimens treated with the solution at pH 4 in the present study. According to the earlier report, the SIMS peak for the $[\text{Cu}(\text{C}_6\text{H}_4\text{N}_3)_2]^-$ species was observed in the mass range of 299-302. In the present study, such shifting was also observed especially in the case of solution at pH 2 as shown in Figure 20. SIMS analysis supports our results obtained from the dissolution study (section , dynamic polishing, electrochemistry and XPS.

From the above discussions, we can conclude that

- It has been found that in the presence of 0.1M glycine, copper removal rate was found to be high in the solution containing 5% H_2O_2 at pH 2 because of Cu-glycine complexation reaction. The dissolution rate of Cu was found to increase due to the formation of highly soluble Cu-glycine complex in the presence of hydrogen peroxide.
- Addition of 0.01M BTA in the solution containing 0.1M glycine and 5% H_2O_2 at pH 2 exhibited a reduction in the Cu removal rate by the formation of Cu-BTA complex on the surface of copper that inhibits the dissolution.
- X-ray photoelectron spectroscopy and secondary ion mass spectroscopy investigations revealed the formation of Cu-glycine complex, which help understand the mechanism of Cu-oxidant-inhibitor interaction during polishing.

From overall discussion in earlier sections, it can be concluded that H_2O_2 is one of the important component of slurry used in Cu-CMP. But, H_2O_2 react vigorously with the polyurethane pad used in the CMP process. Thus there is a need for a new generation pad is originated. Next section addresses this need, the development and the modification of application specific pads which can be successfully used in hydrogen peroxide rich environment.

4.2 Surface Modification of Application Specific Pads (ASP)

Along with the slurry, pads used in Cu-CMP process have direct influence the overall process. CMP polishing pads are cellular polymers, widely known as polymeric foams or plastic. Plasma treatment for polymer surface modification is probably the most versatile among all surface enhancement techniques available till today. The result of near surface (10 – 100 nm) modification can alter a number of chemical and physical properties such as imparting special functional groups for adhesion, hydrophilicity, hydrophobicity, surface energy, chemical inertness, roughness, electrical conductivity, lubricity, cross-linking density, and dyeability. All these properties are important for better application engineering and grafting of polymers.

Plasma modification involves only a few Angstrom top thicknesses, and hence, it does not change the bulk properties of the polymeric materials. Different types of gases used in the plasma such as argon, oxygen, nitrogen, fluorine, and carbon dioxide, which can induce unique properties on the polymeric surfaces. Oxygen plasma treatment can increase the surface energy of polymers, Cross-linking at a polymer surface can also be introduced by inert-gas plasma.

This is the first time in the open literature that surface modification of polymeric pad using the SiO₂ species had been reported to improve the overall CMP process output. Plasma methods used for polymer surface modification are very versatile, the effect ranging from thin film deposition, etching and surface chemical modification.

Plasma enhanced chemical vapor deposition (PECVD) is widely accepted technique for SiO₂ film deposition due to low temperature, fast and high growth rate⁸⁵. The information about the chemical nature of the pad surface resulting from TEOS adsorption and dissociation during PECVD-TEOS treatment was obtained from SEM, XPS, FTIR and nanoindentation analysis. Variation in the coating time of TEOS deposition varies the chemical structure of the pad surface.

Following subsections reports the results of different analysis and discuss their impact.

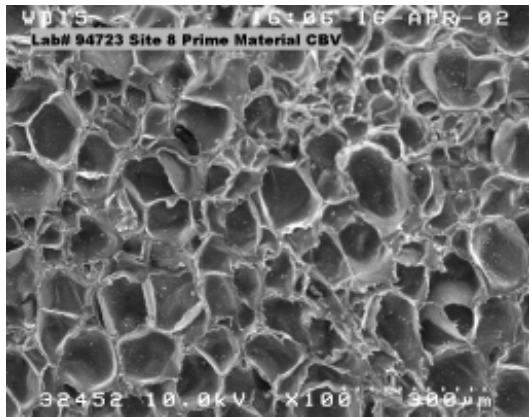
4.2.1 Secondary Electron Microscopy (SEM)

Microstructural characterization of the pad surface before and after coating was compared by visual inspection of the SEM Micrographs. Figure 22 shows the surface morphology of the pad surface before and after coating with the SiO₂ using PECVD technique for the 30 min. The uncoated pad surface found to be smooth, and glassy in appearance. The coated pad was observed to be uniformly coated with few nanometer coating on the surface.

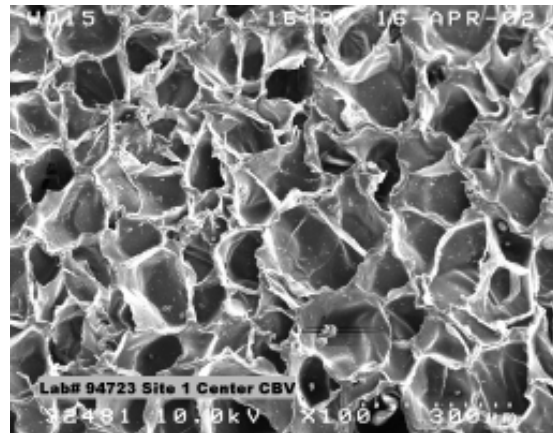
4.2.2 X-ray Photoelectron Spectroscopy

In detail XPS analysis is carried out to deduce chemical changes in pad chemistry with respect to deposition time of TEOS. Data obtained from the XPS analysis include atomic percent ratios, shift in carbon (1s) binding energies, shift in oxygen(1s) binding energies, and ratios of carbon to other elements present on the pad surface.

Pads used in the current study are a grafted polymer as shown in figure 23. In which long chain of polyethylene is grafted by ethylene vinyl acetate. Different materials used for the processing of the polymers.



Uncoated ASP Pad



Coated ASP Pad

Figure 22. Secondary Electron Microscopy images of ASP (a) uncoated; (b) Coated.

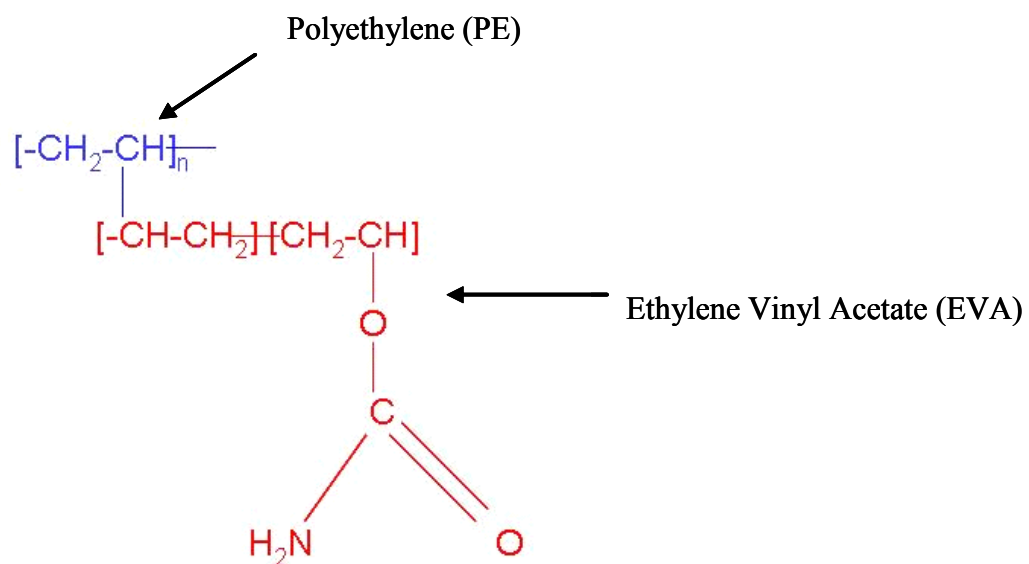


Figure 23. Chemical formula of the polymeric pad

From the initial survey on the sample surfaces it has been seen that along with the carbon, nitrogen and oxygen, silicon is present in all the surfaces.

4.2.2.1 Carbon Binding Energy Shifts

The C (1s) signal was deconvoluted into three major peaks as shown in Figure 24. Deconvoluted XPS C (1s) spectra of PECVD-TEOS treated ASP pad for 10, 20, 30, 40, and 45 min are presented in Figures 24(a), 24(b), 24(c), 24(d), and 24(e), respectively. The peak at the binding energy value of 285.0 eV represents the C-C and C-H functional groups and that observed at 286.5 eV represents the C-O species. These results are in good agreement with the published data. The peak centered at binding energy value of 289.2eV, is attributed to the presence of carbamate functional group [-O-C (NH₂) =O] from the residues of the blowing agent used in the pad substrate manufacturing process. For the specimens coated for 40 and 45 minutes, another XPS peak at binding energy value of 283.8 eV was possibly due to C-Si bond as shown in Figures 24(d) and 24(e)⁸⁶. The binding energy and the full-width-half-maxima (FWHM) values of all carbon peaks are summarized in Table 3.

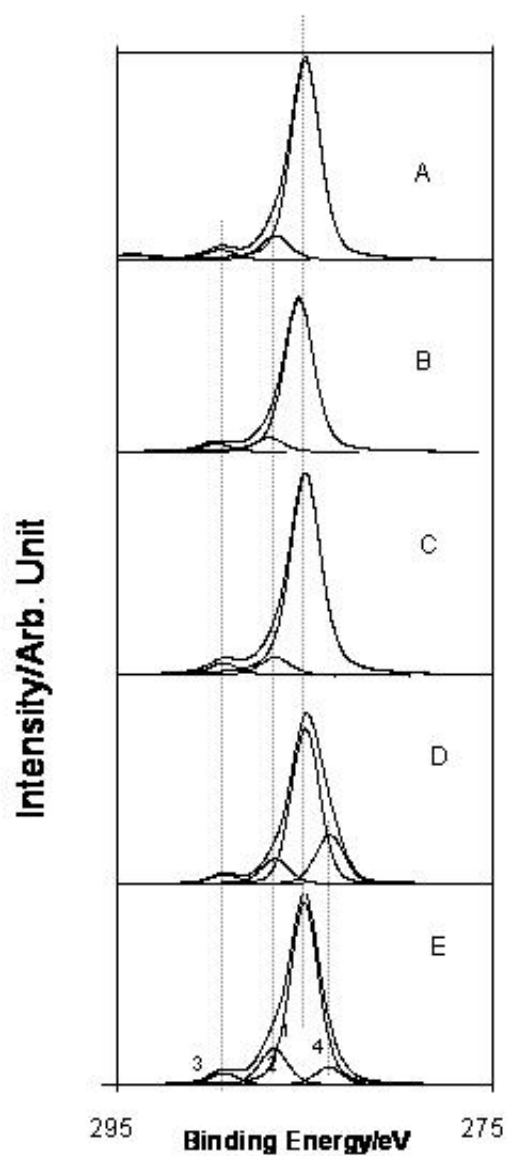


Figure 24. Deconvoluted XPS C (1s) spectra from the ASP surface after PECVD-TEOS treatment for (a) 10min, (b) 20min, (c) 30min, (d) 40min, (e) 45 min. possible peak identification: 1. C-C/C-H, 2. C- O, 3. carbamide, 4. C-Si

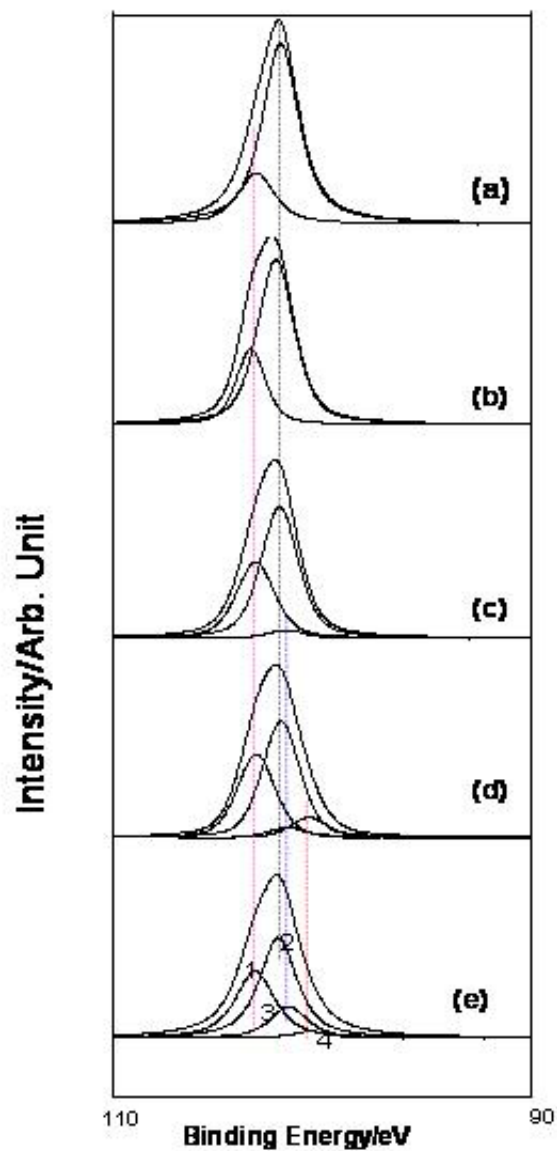


Figure 25. Peak fitted XPS Si (2p) envelop taken from the ASP after TEOS deposition for (a) 10 min, (b) 20 min, (c) 30 min, (d) 40 min, and (e) 45min. possible peak identification: 1. Si-O, 2. Silicate, 3. Si-N, and 4.Si-C.

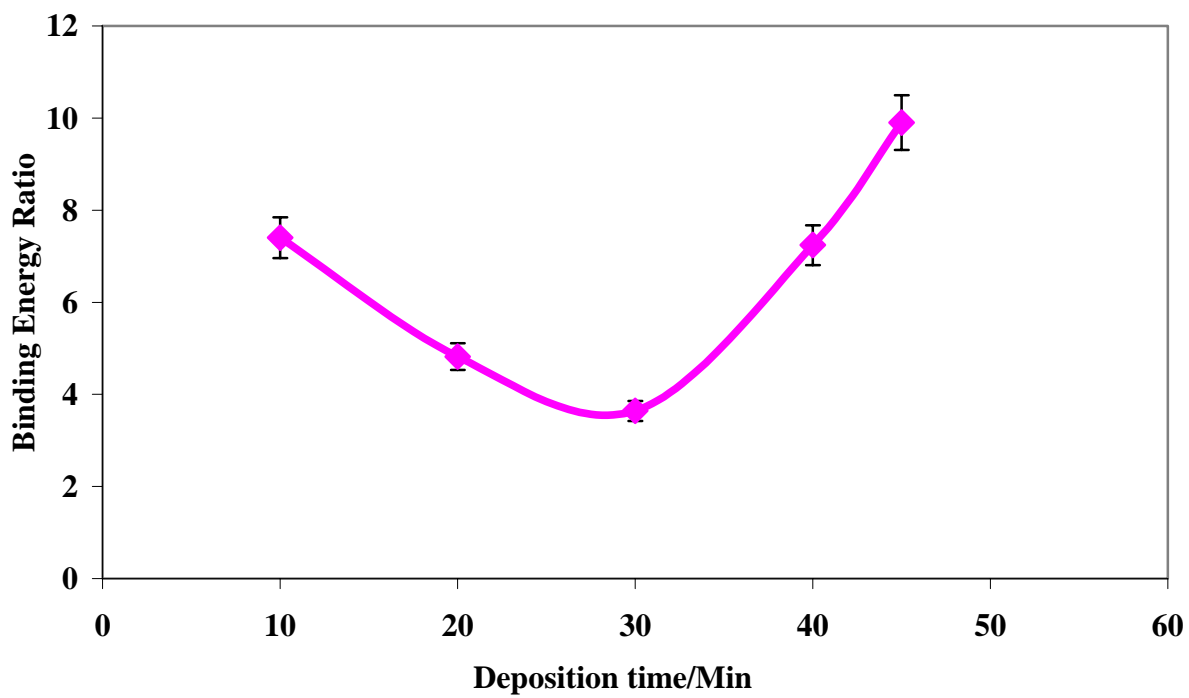


Figure 26. Variation in surface silanol / silicates in PECVD-TEOS coating as a function of deposition time.

Table 3. Variation of composition of XPS C(1s) envelope as a function of PECVD treatment time with TEOS on the top surface of ASP pads.

Duration of PECVD/min	XPS C(1s) peak parameters and corresponding functional groups		
	Binding Energy/eV (± 0.1 eV)	FWHM/eV (± 0.05 eV)	Functional Group
10	285.0	1.70	C-C / C-H
	286.5	1.70	C-O
	289.2	1.70	-O-C(NH ₂)=O
20	285.0	1.73	C-C or C-H
	286.5	1.73	C-O
	289.2	1.73	-O-C(NH ₂)=O
30	285.0	1.78	C-C / C-H
	286.5	1.78	C-O
	289.2	1.78	-O-C(NH ₂)=O
40	285.0	1.65	C-C / C-H
	283.8	1.65	C-Si
	286.5	1.65	C-O
	289.2	1.65	-O-C(NH ₂)=O
45	285.0	1.68	C-C / C-H
	283.8	1.65	C-Si
	286.5	1.65	C-O
	289.2	1.65	-O-C(NH ₂)=O

4.2.2.2 Silicon Binding Energy shifts

Deconvolution of XPS Si (2p) envelope obtained from the pad specimens PECVD treated up to 30 minutes revealed two major peaks at 102.3 and 103.4 eV, representing silicate and Si-O species, respectively. The peak fitted Si (2p) envelopes for specimens that were PECVD treated for 10, 20, 30, 40, and 45 minutes, are depicted in Figure 25. The data indicate that short PECVD process time produced surface films rich in silanol (Si-OH), consistent with TEOS films deposited at lower process temperatures⁸⁷. At the initial stages of deposition greater numbers of hydrogen atoms are incorporated into the film and react with the oxygen species on the pad surface to form more Si-OH. Due to the increase in Si-OH content the porosity of the film increases and in turn, the density of the SiO₂ film decreases. Figure 26 shows the oxygen to silicon (O/Si) stoichiometry ratio values calculated from the XPS data using equation (4). The ratio is proportional to the concentration of the silanol in the deposited coatings. Fracassi *et al.* have shown that as substrate temperature increases, hydrogen content in the film decreases and the film becomes rich in SiO₂ having dense structure. The O/Si ratio again starts increasing after 30 min deposition time due to higher concentration of oxygen on the surface and subsequent reduction in silicon species. For the PECVD specimens treated for 30, 40 and 45 min, a small peak was observed at 102.1 eV, which represents Si-N bond. Furthermore, there is an abrupt reduction in Si to N stoichiometry ratio, which indicates an increase in the nitrogen species on the surface. These observations suggest that as the deposition time increases, thermal energy of the depositing species increases, atomic vibrations probably occur, which result in breaking the bonds between species on the pad surface. Consequently, the material etches out from the substrate. The nitrogen reacts with the Si species on the pad surface, forming Si₃N₄ species in stoichiometric conversion from SiO₂ to Si₃N₄⁸⁸.

At longer coating times, the ion bombardment on the foam surface generates appreciable amounts of reactive carbon radicals on the surface of the pad. Such radicals possibly reacted with the silicon species to form silicon carbide (SiC), which was subsequently incorporated into the surface coating of the pad. An XPS peak at 101 eV was observed, as shown in Figure 25, which confirms the presence of such SiC species. The incorporation of Si₃N₄ and SiC species would certainly be expected to make the pad surface stiffer and more brittle.

4.2.3 Fourier Transform Infrared Spectroscopy

Transmittance plot of surface ATR-FTIR signal through TEOS coated PE-EVA foam substrate as a function of coating time is shown in Figure 27. The plots in Figure 25 are of the IR transmittance associated with the asymmetric Si-O-Si stretch of silica ($\nu = 1010 \text{ cm}^{-1}$) and the Si-O-X stretch ($\nu = 950 \text{ cm}^{-1}$), respectively. There is a monotonic net decrease in the surface concentration of Si-O moieties with PECVD time, as reflected in the increased transmittance up to 30 minutes of coating time. Thereafter, it appears to be a change in the deposition kinetics, consequently, decrease in the concentration of both Si-O-Si and Si-O-X (where X is H, C) was observed. Such observation is inconsistent with generally accepted TEOS deposition mechanisms and kinetics. The concentration of Si-O-Si and Si-O-X, species is expected to increase with TEOS deposition time on other substrates^{87,89,90}. However, in the present situation, the concentration of such species was decreased with the duration of PECVD; possibly due to the degradation of the polymeric pad, and forming silicon carbide and silicon nitride.

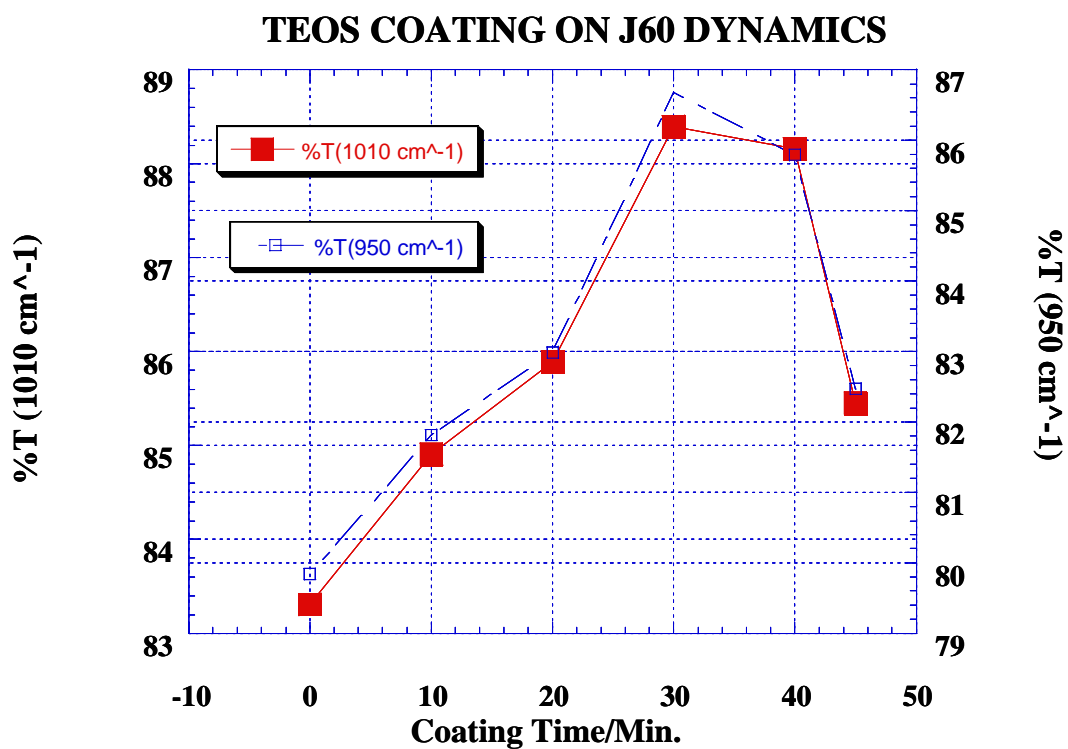


Figure 27. Transmittance plot of surface ATR-FTIR signal through TEOS coated polyethylene-ethylene vinyl acetate (PE-EVA) foam substrate as a function of coating time.

4.2.4 Nanoindentation

The load-depth (P-h) curves obtained from the nanoindentation were analyzed using Oliver-Pharr approach. The specimens exhibited a non-uniform penetration during the indentation experiments. Qualitative examination of the P-h curve showed some unique characteristics. As shown in Figure 28, distinct events such as pop-in, pop-out or kink-back, were clearly discernible from the curves. The presence of pop-in during the loading cycle was observed with a characteristic sudden penetration of the indenter into the specimen without an increase of the load. On the other hand, pop-out was observed during unloading cycle with a characteristic of a sudden withdrawal of the indenter without any change in the load. Such events were found to correlate with several experimental parameters, such as coating time, loading/unloading rate and depth of indentation. Further nanoindentation study of the PECVD treated pads revealed that pop-in events occurred more often for indenter penetration depths around 1000 nm. Although pop-out events were not affected by the depth of indentation, rate of loading and unloading has significant influence on both the events. These events also indicate the extent of plastic deformation of the pads during nanoindentation. It is well known that the plastic deformation is a critical attribute of CMP pads as it affects the efficiency of the CMP process and therefore, the presence of such events in the load-depth curves indicates an improved performance.

Further analysis of the P-h curves obtained from the indentation test of specimens with varying coating time revealed that there exist a drop in the loading curve after a sharp increase at the initial loading period. The depth at which such transition in the loading curve occurs is denoted as h_{tr} . Figure 29 shows the correlation between the transition depth and PECVD-TEOS coating time, which reveals that the transition depth increases with the coating time. Such trends are possibly attributed to the change of thickness of the plasma modified layer on the top surface of the ASP pad with coating time. The slope of P-h prior to the transition depth was found to be higher than that beyond

the transition depth. Such results strongly suggest an improvement in the mechanical properties of the top surface of the pad due to PECVD treatment. Figures 30 and 31 depict the effect of coating time on the hardness and elastic modulus of the pad material, respectively. The effective surface modulus and hardness were found to increase with increasing PECVD-TEOS coating time. Since the substrate is made of closed-cell foam, it is unlikely that the reactive TEOS-derived species diffuse into the bulk. The changes in the mechanical properties of the pad surface are clearly due to the effect of the coating deposited on the foam substrate. Unlike the values of hardness and elastic modulus, the percent of transmittance of ATR-FTIR signal was found to decrease after 30 minutes of PECVD coating time as shown in Figure 27, which was possibly due to the changes in the pad surface chemistry rather than net removal of the TEOS-derived coatings.

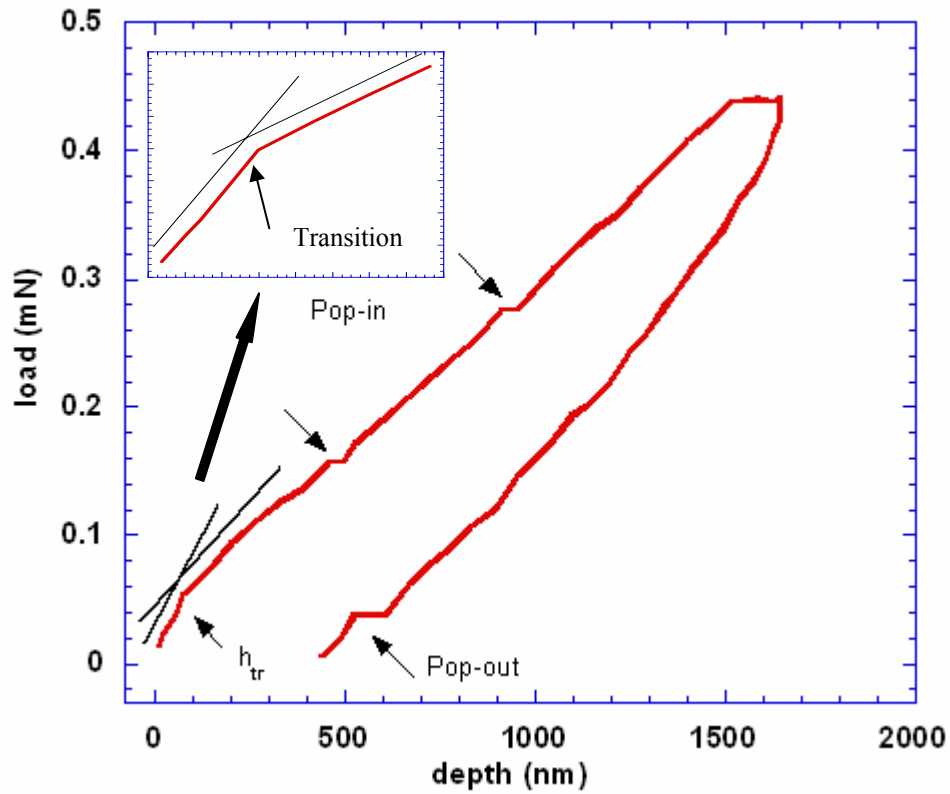


Figure 28. Load-penetration behavior of CMP pads during nanoindentation on pad PECVD treated for 45 min. Inset: The slope change at the transition point at a depth of h_{tr} .⁹¹

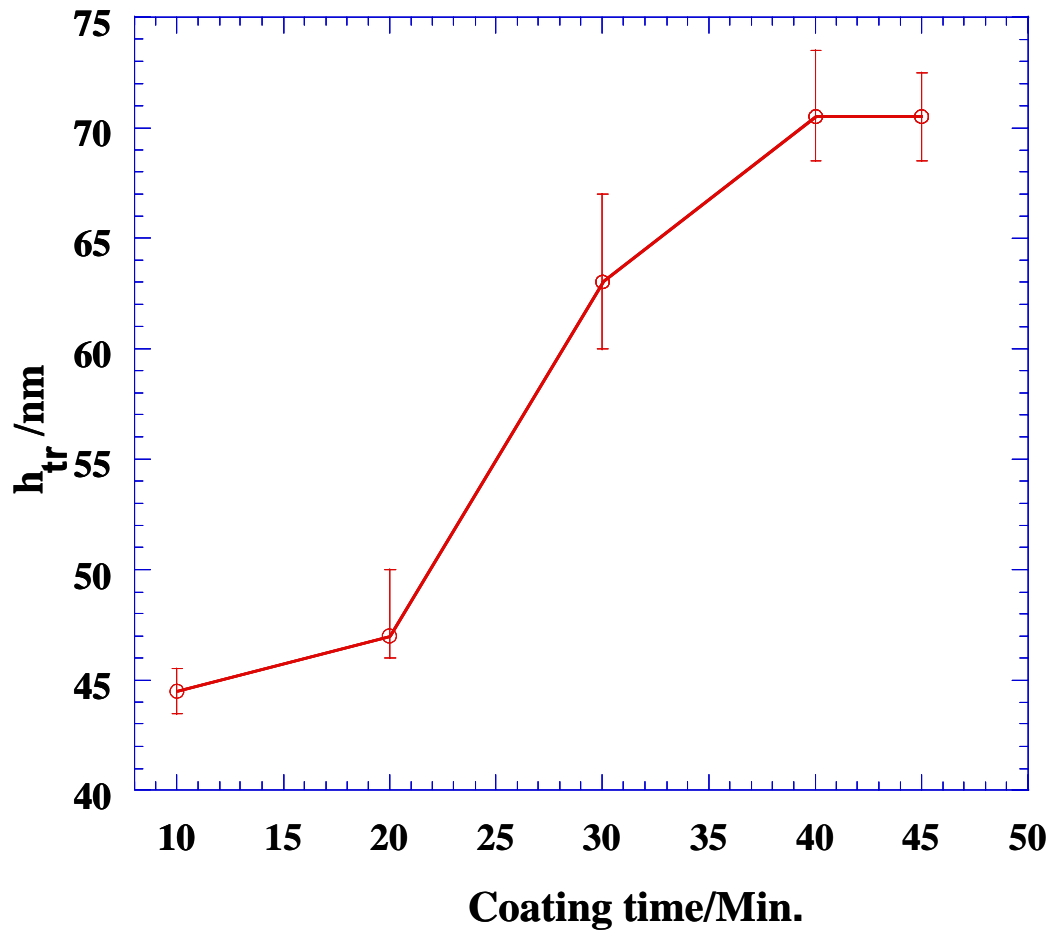


Figure 29. Variation of transition depth (h_{tr}) as a function of PECVD-TEOS coating time during nanoindentation tests.

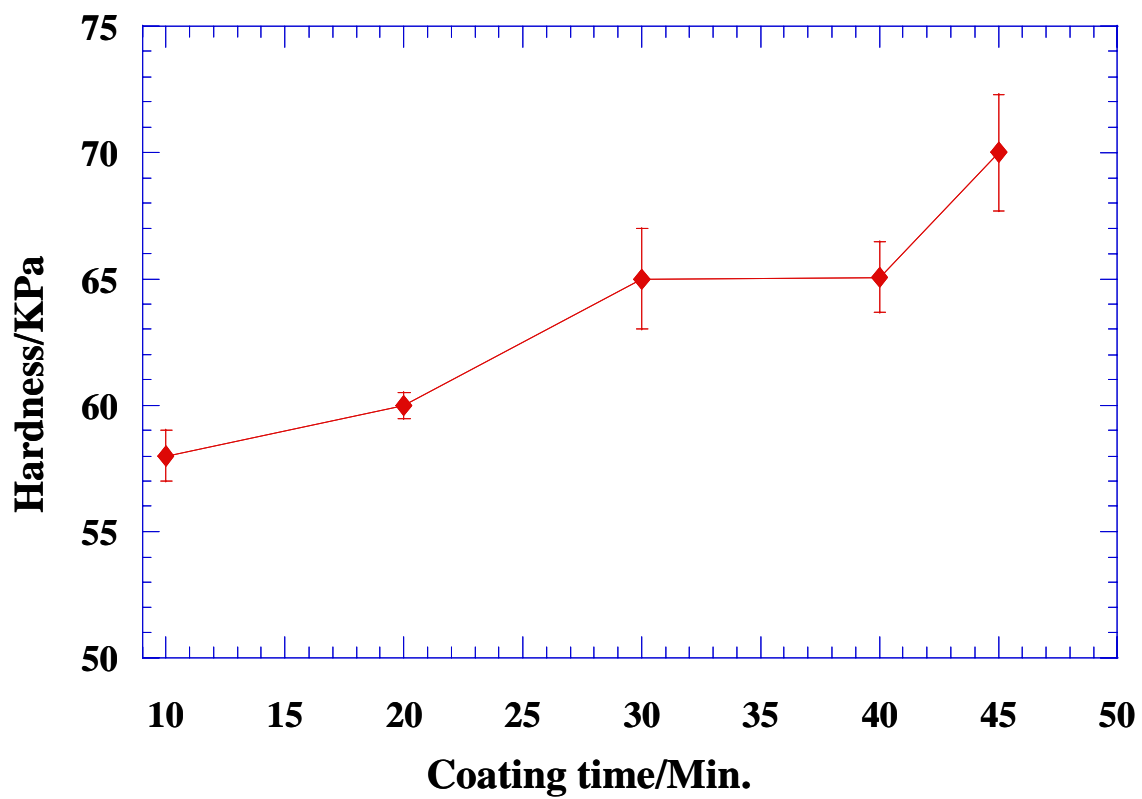


Figure 30. Hardness as a function of PECVD-TEOS coating time.

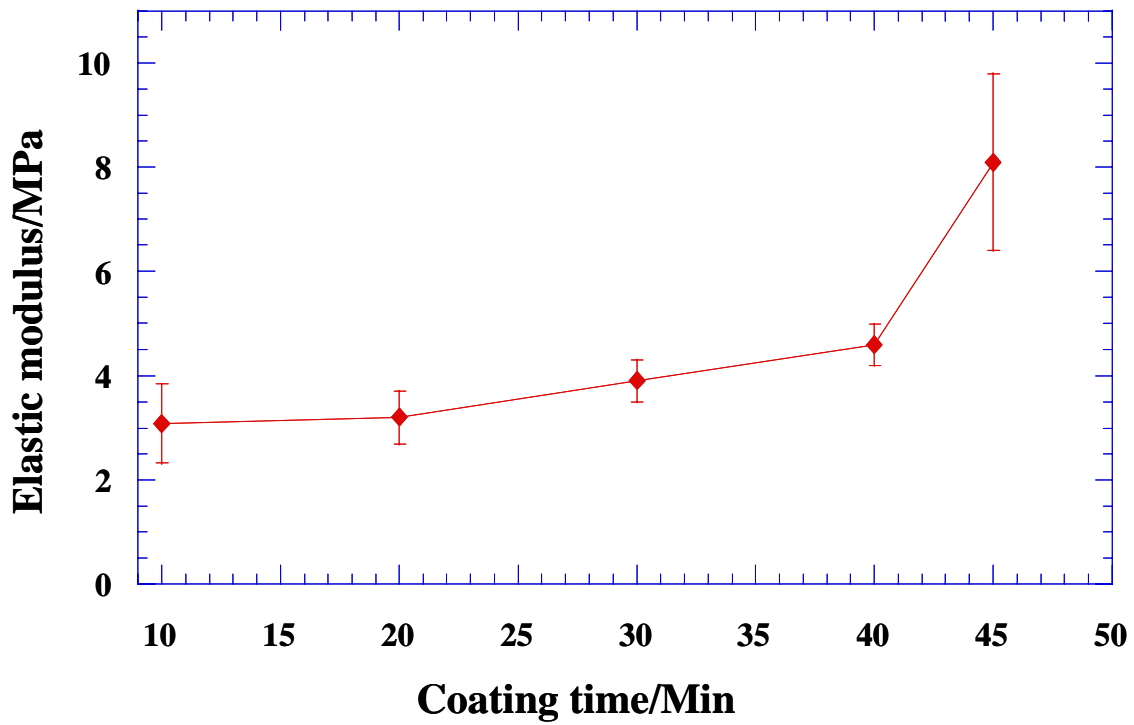


Figure 31. Elastic modulus as a function of PECVD-TEOS coating time.

4.2.5 Correlation of ATR-FTIR, XPS and Nanoindentation Results

The ATR-FTIR results suggest PECVD TEOS on foams is a rather complex deposition process, involving competition among several elementary processes. The PECVD-TEOS coating process produces both silica and silicates on the foam surface. The XPS results show changes in the surface chemistry of the substrate as a function of deposition time at a fixed TEOS/O₂ mixture. The formation of SiO₂, SiC, and Si₃N₄ perhaps alters the viscoelastic properties of the foam surface, leading to enhanced stiffness, hardness, modulus of elasticity. It can be mentioned that the mechanical behavior of the PECVD treated pads, as observed by nanoindentation studies, correlates the FTIR and XPS results in the present study. At shorter deposition time, a gradual monotonic increase in surface hardness and modulus of elasticity was observed. However, beyond 30 minutes of PECVD treatment, a sudden change in the hardness and elastic modulus was observed which was due to the incorporation of Si₃N₄ and SiC into the surface coatings, as observed in the XPS study.

4.2.6 Impact of Pad Surface Modifications on Polishing Performance

To study the effect of PECVD coating on pad surface dynamic polishing studies has been carried out. In a typical CMP setup, tungsten wafer is used and polishing is carried out.

Figure 32 represents the relative blanket tungsten removal rate (W-RR) as a function of PECVD coating time. It can be observed from figure as thickness of the PECVD-TEOS coating increases W removal rate also increases. As discussed before, the surface chemistry of pad changes with coating time. The study enabled us to design ASP pads with the following characteristics: no need for the traditional pad 'break-in' before polish, no conditioning/dressing ever, no need to keep pads wet in idle mode, long pad life, high selectivity, ergonomically friendly/easy pad changes and demonstrated pad-to-pad reproducibility.

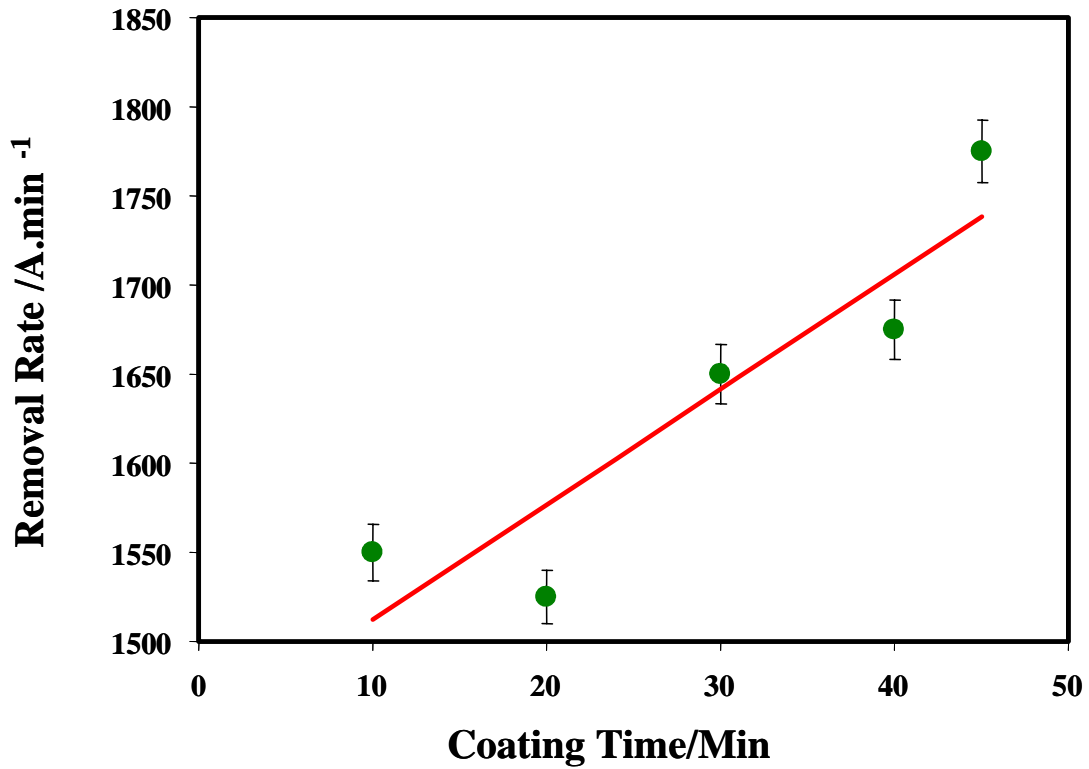


Figure 32. Correlation of relative blanket tungsten removal rate (W-RR) and PECVD-TEOS coating time.

CHAPTER 5. CONCLUSION

Interaction between Cu-glycine-H₂O₂-benzotriazole in Cu-CMP as well as surface modification of CMP application specific pads have been successfully studied using different characterization techniques. From this study we can conclude that:

1. Copper (Cu)- removal rate in pH 2 solution in the presence of 0.1M glycine was found to be highest for 5% H₂O₂ concentration. Removal rate of Cu is increased due to the formation of highly soluble Cu-glycine complex.
2. In presence of glycine at same hydrogen peroxide concentration higher dissolution rate is observed at pH 2.
3. Increase in the H₂O₂ concentration above 5% decreases the Cu dissolution rate in pH 2 solution, possibly because of hydroxyl ion generated during the oxidation process decreases the driving force for Cu dissolution.
4. Glycine showed higher efficiency at 0.1M concentration.
5. In this system addition of 0.01M BTA effectively reduces Cu removal rate via formation of Cu-BTA complex on the surface of Cu, inhibiting the dissolution rate.
6. The inhibition efficiency of BTA of Cu dissolution in solution containing 0.1M glycine and 5%H₂O₂ is decreased at lower pH solution.
7. The tuning of the chemical and mechanical properties of the top surface of the Application specific pads (ASP) using plasma enhanced chemical vapor deposition of tetraethyl orthosilicate is feasible.

8. The modification of mechanical properties of the pad top surface is a function of the duration of the plasma enhanced chemical vapor deposition. The metal removal rate using such surface modified polishing pad was found to increase linearly with the duration of plasma enhanced chemical vapor deposition.
9. The gradual enhancement of hardness and modulus of elasticity of the PECVD-TEOS pad at the initial period was due to the formation of silicate and silica species. However, the polymer pad degrades beyond 30 minutes of deposition, and lead to the formation of silicon carbide and silicon nitride species as evident from the XPS studies.
10. Initially a sharp change in the mechanical properties of the pad surface was quantified by monitoring the change of slope in the load-penetration curve. The depth at which such transition of mechanical properties takes place is a function of PECVD deposition times.

CHAPTER 6. IMPACT OF CURRENT RESEARCH AND FUTURE

TRENDS IN METAL CMP

For most of the wafer manufacturing processes the cost of processing wafers is controlled by the equipment utilization and the cost of the equipment. In case of metal CMP, cost of the slurry is one of the greatest contributors to the cost of processing wafers. Morrison *et al.* mentioned that the total cost of the consumables is around 50 to 70 % of overall cost and especially the slurry can be around 40% of the Cost of Ownership (CoO).

The main finding of this study is aimed to optimize the slurry used in the Cu-CMP. Since high dissolution rate are observed without the abrasives which significantly reduce post CMP cleaning as well as loss of the wafers due to scratching. At the same time other major contributor to the CMP CoO is, of course, the CMP pad itself. The new pad can have a significantly different removal rate from the replaced pad, a time-consuming re-qualification process is thus necessary. The application specific pads (ASP) are produced and surface modified by a unique manufacturing process. They are significantly different from the currently used solid polyurethane pads. This ASP greatly reduces the pad-to-pad non-uniformity, and consequently can lead to the reduced pad re-qualification time. Increased pad life (the number of wafers each pad can polish) is a function of optimized pad conditioning and the amount of pad damage during the polish and the conditioning process. Current research on the Application Specific Pads (ASP) indicates that the minimal conditioning is required to maintain consistent removal rates from one wafer to the next. From all above discussion we can conclude that the

finding of this thesis will help to reduce the cost of the overall CMP process, as shown in figure 33.

At the same time overall Chemical Mechanical Planarization phenomenon occurs at atomic level and removal of metal layers is in the nanoscale. Nanotechnology is an emerging area of modern science, which concerns itself with the study of materials that have very small dimensions. Application of nanotechnology to the CMP is also a new area of research. Scientists and technologists are deeply involved to understand the novel properties of materials in nano dimensions and their enable applications in CMP. Nanotechnology requires a fundamental understanding of how nature works at the atomic scale. Nature has the ability to design highly energy efficient systems that operate precisely and without waste, fix only that which needs fixing, do only that which needs to be done, and nothing else. Our understanding of nanoscale phenomena may allow us to replicate at least part of what nature accomplishes with ease.

Nanoparticles suspended into the slurry can act as an abrasives in CMP. Smaller abrasive particle sizes enable the semiconductor industry to maintain quality control while shrinking the size of their chip designs in the drive to lower cost per chip. This establishes a new benchmark for slurry and pad production in the CMP market and is an important development for the newer chip fabrication technologies.

Alumina (Al_2O_3), Silicon dioxide (SiO_2), Ceria (CeO_2) and Zirconia (ZrO_2) are some of the most widely used abrasives in the CMP industry. Dr. Seal's research group at Surface engineering and Nanotechnology Facility (SNF) laboratory extensively working on synthesis and characterization of nanoparticles, especially rare earth oxide nanoparticles.

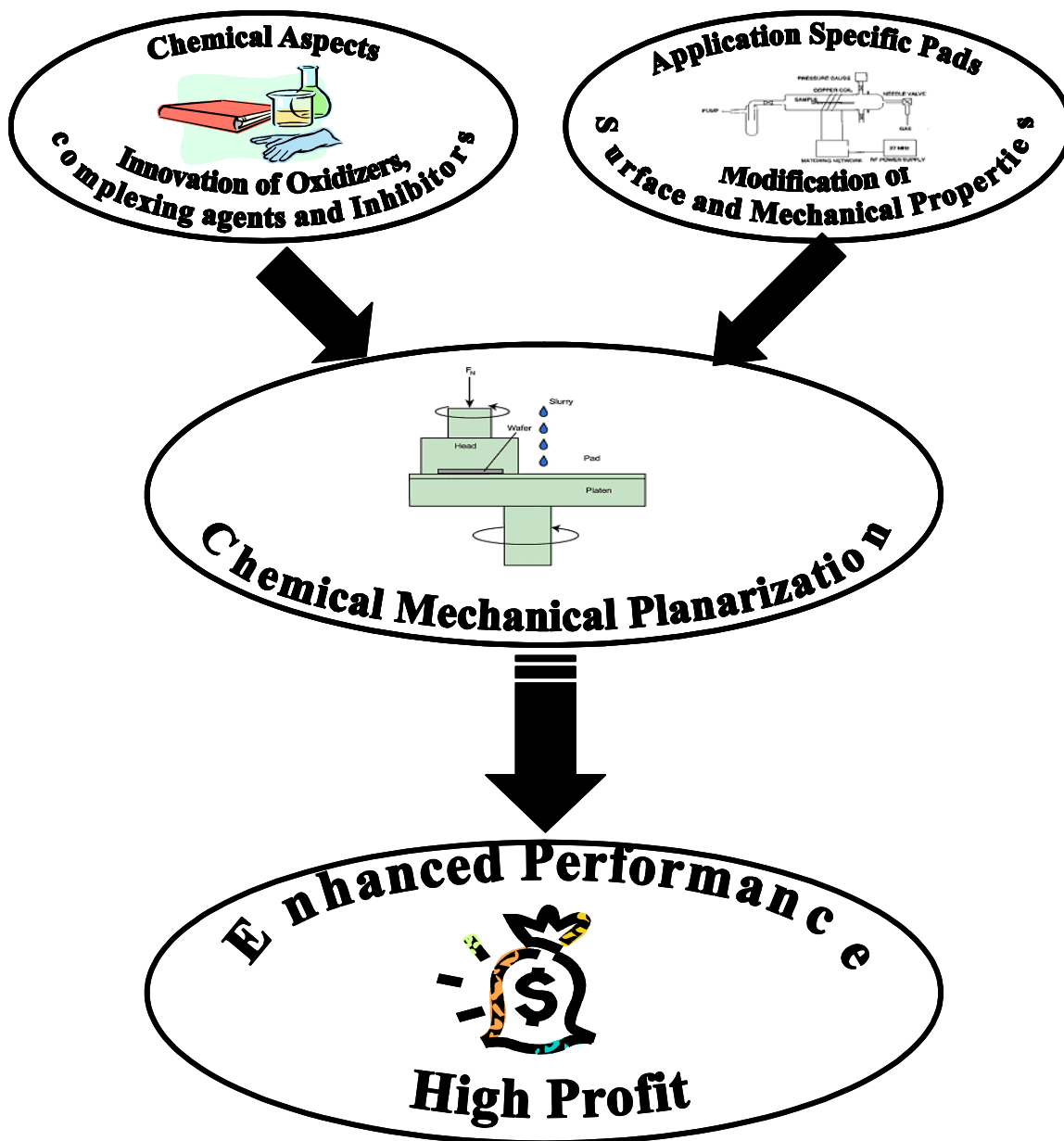


Figure 33. Impact of current research on chemical mechanical planarization industry.

Nanocrystalline Cerium oxide is one such example and shows some interesting properties. It acts as a good radical scavenger in oxygen rich environment while in lean oxygen environment it releases oxygen. This can be act as an abrasive and oxidizer. Use of such kind of nanoparticles may overcome the need of use of oxidizing agent in to the CMP process which ultimately reduces the CoO.

Presently some initial studies have been conducted with the particles in presence of glycine in copper CMP. Initial results are encouraging and indicate the active dissolution of copper in the solution in presence of the nanoparticles. Further studies in this area are currently in progress and the work will be concluded in subsequent years.

APPENDIX: PUBLICATIONS

- S.Deshpande, S.C.Kuiry, M.Klimov, Y.Obeng , and S.Seal, “Chemical Mechanical Polishing of copper: Role of oxidants and Inhibitors”, Journal of Electrochemical Society, *In Press*
- S.Deshpande, S.Dakshinamurthy, S.C.Kuiry, R.Vaidyanathan, Y.Obeng and S.Seal. “Surface modification of polymeric pads for enhanced performance of chemical mechanical polishing of copper”, Thin Solid films, *Under Review*.
- Y.Obeng, J.E. Ramsdell, S.C.Kuiry,K.Chamma, K.Richardson, S.Deshpande, and S.Seal “Impact of CMP consumables on copper metallization reliability”, *IEEE, Under review*.
- S.C.Kuiry, S.Deshpande, M.Klimov, Y.Obeng and S.Seal, “Chemical Mechanical Polishing of copper: Role of oxidants and Inhibitors” in “Chemical Mechanical Planarization VI”, S.Seal, R.L.Opila, K.B.Sundaram, and R.Singh, The Electrochemical Society Proceeding volume-VI, ISBN 1-56677-404-7Orlando, Florida (2003) p.52
- Y.Obeng, K.Chamma, S.Deshpande,S.C.Kuiry,R.Vaidyanathan,K.Richardson,and S.Seal, “ Performance- Surface characteristics of PsiloQuest’s Application Specific Pads for Chemical Mechanical Polishing” in “Chemical Mechanical Planarization VI”, S.Seal, R.L.Opila, K.B.Sundaram, and R.Singh, The Electrochemical Society Proceeding volume-VI, ISBN 1-56677-404-7Orlando, Florida (2003) p.126.

LIST OF REFERENCES

- ¹ G.E.Moore, “Cramming more component onto electronics circuit”, *Electronics* 38 (1965) 21.
- ² C.I.Borst, W.N.Gill, R.J.Gutman, “Chemical –Mechanical Polishing of low dielectric constant polymers and organosilicate glasses”, Kluwer Academic Publishers, Boston (2002).
- ³ J.M.Steigerwald, S.P.Murarka, R.J.Gutman, “Chemical Mechanical Planarization of Microelectronic Materials”, John-Weley & sons Inc., NewYork (1998).
- ⁴ C. Steinbrüchel, “Patterning of copper for multilevel metallization: reactive ion etching and chemical-mechanical polishing”, *Appl. Surf. Sci.* 91 (1995) 139.
- ⁵ J. M.Steigerwald, S.P.Murarka, R.J.Gutmann, D. Duquette, “Chemical processes in the chemical mechanical polishing of copper”, *Mater.Chem.Phys.* 41 (1995) 217.
- ⁶ H. Mavoori, “Copper/Low-k interconnects for smaller and faster circuits”, *JOM* 26 (1999) 36.
- ⁷ The National Technology Roadmap for Semiconductor, Semiconductor Industry Association (SIA), San Jose, CA (1998).
- ⁸ T.N. Theis, “The future of interconnection technology”, *IBM J. Res. Develop.* 44 (2000) 379.
- ⁹ M.Morgen,E.Todd Ryan, J.H. Zhao, C.Hu,T.Cho, P.S.Ho, “ Low dielectric constant materials for advanced interconnects” *JOM* 51 (1999) 37.
- ¹⁰ S.P Murarka “ Future challenges in CMP” in *Chemical-Mechanical Polishing–Fundamentals and Challenges*, S. V. Babu, S. Danyluk, M. I. Krishnan, and M. Tsujimura, Editors, p. 3 , Materials Research Society, San Francisco, CA (1999).

-
- ¹¹ L.Zhang, S.Raghavan, M.Weling, “Minimization of chemical-mechanical planarization (CMP) defect and post-CMP cleaning”, *J. Vac. Sci. Technology B* 17 (1999) 2248.
- ¹² M.Oliver, “CMP fundamentals and challenges”, in *Chemical-Mechanical Polishing—Fundamentals and Challenges*, S. V. Babu, S. Danyluk, M. I. Krishnan, and M. Tsujimura, Editors, p. 73 , Materials Research Society, San Francisco, CA (1999).
- ¹³ Z.Stavreva, D. Zeidler, M. Plotner, G. Grasshoff, and K. Drescher, “Chemical mechanical polishing of copper for interconnect formation”, *Micro Engg.* 33 (1997) 249.
- ¹⁴ R.Bajaj,F.Redeker,K.Wijekoon, “ Unlocking copper damascene puzzle”, in *Interconnect Status*, Semicon West, San Francisco, CA (2000).
- ¹⁵ K. Wijekoon,S. Tsai,D. Bennett, and F. Redeker, “ An investigation on the characterization of chemical mechanical polishing of copper”, in *Chemical-Mechanical Polishing in IC device manufacturing III* , Y. A. Arimoto, R. L. Opila, C. Reidsema Simpson, K. B. Sundaram, I. Ali, and Y. Homma, Editors, p.158, The electrochemical Society , Honolulu, HI (1999).
- ¹⁶K.Wijekoom, S.Tsai, M.Chandrachood, B.Brown, F.Redeker, S.Nanjangud, G.Amico, “Multistep approach to copper development”, in Technical Symposium *SEMI*, Japan (1998).
- ¹⁷ B.Morisson, S.Joshi, R.Tolles, “Copper and STI CMP Technology: The challenges and the cost” , *Future Fab. Intl.* 11 (2000).
- ¹⁸ L. Peters, “ Choices and challenges for shallow trench isolation”, *Semi.Intl.* 4 (1999) 2121.
- ¹⁹ R.Tiwari,M.Soucek, J.Strupp, “Development and implementation of 300 mm Cu CMP manufacturing system” , *Future Fab. Intl.* 12 (2003) 546.
- ²⁰ A.K. Sikder, I.M. Irfan, A.Kumar, a. Belyaev, S.Ostapenko,M.Claves, J.P Harmon, J.M.Anthony, “ Evaluation of mechanical and tribological behavior, and surface characteristics

of CMP pads” , in *Chemical-Mechanical Polishing 2001 –Advances and future challenges* , S. V. Babu, K.C.Cadien, and H.Yano, Editors, p. M 1.8.1 , Materials Research Society, San Francisco, CA (2001).

²¹ Y.Kamigata, Y.Kurata, K.Masuda, J.Amanokura, M.Yoshida, M.Hanazono, “Why abrasive free Cu slurry is polishing” , in *Chemical-Mechanical Polishing 2001 –Advances and future challenges* , S. V. Babu, K.C.Cadien, and H.Yano, Editors, p. M 1.3.1 , Materials Research Society, San Francisco, CA (2001).

²² T. Du ,V. Deasai, “The pH Effect on Chemical Mechanical polishing of copper”, in *Chemical-Mechanical Planarization*, D.Boning, K. Devriendt,M.Oliver,D.Stein, and I.Vos , Editors, p. F 6.6 , Materials Research Society, San Francisco, CA (2003).

²³ A.Jindal,Y.Li,S.V.Babu , “Effect of pH on chemical mechanical polishing of copper and tantlum”, in *Chemical-Mechanical Polishing 2001 –Advances and future challenges* , S. V. Babu, K.C.Cadien, and H.Yano, Editors, M 6.8.1 , Materials Research Society, San Francisco, CA (2001).

²⁴ W.Huang, S. Tamilmani, S. Raghavan, R.Small, “ Dissolution of copper thin films in hydroxylamine-based solutions”, *Intl. J. Mineral Proc.* 72 (2003) 365.

²⁵ S. Seal, S. C. Kuiry, and B. Heinmen, “ Effect of glycine and Hydrogen peroxide on chemical mechanical polishing of copper”, *Thin Solid Films* 423 (2003) 243.

²⁶ F.B.Kaufman, D.B. Thomson,R.E. Broadie,M.A. Jaso,W.L Gutherie, D.J. Peterson, M.B. Small, “Chemical-mechanical polishing for fabricating Patterned W metal features as chip interconnect”, *J. Electro. Soc.* 143 (1996) 3041.

-
- ²⁷ J.M. Steigerwald, S.P. Murarka, J. Ho, R.J. Gutman, and D.J. Duquette, "Mechanisms of copper removal during chemical mechanical polishing", *J. Vac. Sci Tech B* 13 (1995) 2215.
- ²⁸ Q. Luo, D. R. Campbell, and S. V. Babu, "Stabilization of alumina slurry for chemical-mechanical polishing of copper", *Langmuir* 12 (1996) 3563.
- ²⁹ M. T. Wang, M. S. Tsai, C. Liu, W. T. Tseng, T. C. Chang, L. J. Chen, and M. C. Chen, "Effect of corrosion environment on the surface finishing of copper chemical mechanical polishing", *Thin Solid Films* 308/309 (1997) 518.
- ³⁰ Q. Luo, S. Ramarajan, and S. V. Babu, "Modification of the preston equation for the chemical-mechanical polishing of copper", *Thin Solid Films* 335 (1998) 160.
- ³¹ M. Fayolle, and F. Romagna, "Copper CMP evaluation: planarization issues", *Microelectronics Engg.* 37/38 (1997) 135.
- ³² M. Hariharaputhiran, S. Ramarajan, Y. Li, and S. V. Babu, "Mechanism of Cu removal during CMP in H₂O₂-glycine based slurries" in *Chemical-Mechanical Polishing—Fundamentals and Challenges*, S. V. Babu, S. Danyluk, M. I. Krishnan, and M. Tsujimura, Editors, p.129, Materials Research Society, San Francisco, CA (2000).
- ³³ Y. Luo, T. Du, V. Desai, "Chemical Mechanical planarization of copper: the effect of inhibitors and complexing agents", in *Chemical-Mechanical Planarization*, D. Boning, K. Devriendt, M. Oliver, D. Stein, and I. Vos, Editors, p. F 6.10, Materials Research Society, San Francisco, CA (2003).
- ³⁴ K. Osseo-Asare, K.K. Mishra, "Solution chemical constraints in the chemical-mechanical polishing of copper: Aqueous stability diagrams for the Cu-H₂O and Cu-NH₃-H₂O Systems", *J. Electro. Matl.* 25 (1996) 1599.

-
- ³⁵ Q.Luo, R.A.Mackay, S.V.Babu, “ Copper dissolution in aqueous ammonia-containing media during Chemical Mechanical polishing” , *Chem. Matl.* 9 (1997) 2101.
- ³⁶ Y.Ein-Eli, E.Abelev, D.Starosvetsky, “ Electrochemical aspects of copper chemical mechanical planarization (CMP) in peroxide based slurries containing BTA and glycine” , *Electro. Acta* 49 (2004) 1499.
- ³⁷ R.B.Faltermeier , “ A corrosion inhibitor test for copper-based artifacts” , *Studies in Conser.* 44 (1998) 121.
- ³⁸ R. Walker, “Triazole,Benzotriazole and Nephthotriazole as corrosion inhibitors for copper” , *Corrosion* 31 (1975) 97.
- ³⁹ T. Notoya, and G. Poling, “Topographies of thick Cu-Benzotriazole films on Copper” , *Corrosion* 32 (1976) 216.
- ⁴⁰ M. Ito, and M. Takahashi, “IR reflection-absorption spectroscopic study of benzotriazole on copper” *Surf. Sci.* 158 (1985) 609.
- ⁴¹ S. L. Cohen, V. A. Brusic, F. B. Kaufman, G. S. Frankel, S. Motakef, and B. Rush, “X-ray photoelectron spectroscopy and ellipsometry studies of the electrochemically controlled adsorption of benzotriazole on copper surfaces” , *J. Vac. Sci. Tech. A* 8 (1990) 2417.
- ⁴² V. Brusic, M. A. Frisch, B. N. Eldridge, F. P. Novak, F. B. Kaufman, B. F. Rush, and G. S. Frankel, “Copper corrosion with and without inhibitors” *J. Electrochem. Soc.* 138 (1991) 2253.
- ⁴³ R. Thomas, V. Brusic, and M. Rush, “Correlation of surface wettability and corrosion rate for benzotriazole treated copper” , *J. Electrochem. Soc.* 139 (1992) 678.

-
- ⁴⁴ L. Tommesani, G. Brunoro, A. Frignani, C. Monticelli, and M. Dal Colle, “On the protective action of 1,2,3-Benzotriazole derivative films against copper corrosion” *Corrosion Sci.* 39 (1997) 1221.
- ⁴⁵ J. Walsh, H. Dhariwal, A. Gutierrez, P. Finneti, C. Muryn, N. Brookes, R. Oldman, and G. Thornton, “Probing molecular orientation in corrosion inhibition via a NEXAFS study of benzotriazole and related molecules on Cu (100)” *Surf. Sci.* 415 (1998) 423.
- ⁴⁶ A.L.Roy, J.L. Checchi, D.L. Hetherington, D.J. Stein, “Polyurethane pad degradation and wear due to tungsten and oxide CMP”, in *Chemical-Mechanical Polishing 2001 –Advances and future challenges*, S. V. Babu, K.C. Cadien, and H. Yano, Editors, M1.7.1, Materials Research Society, San Francisco, CA (2001).
- ⁴⁷ T. Kelen, “Polymer Degradation”, Pubs Van Noster and Reinhold Company, New York (1983).
- ⁴⁸ K. Nakamura, S. Kishii and Y. Arimoto, “Reconditioning-Free Polishing for Interlayer-Dielectric Planarization”, *Jpn. J. Appl. Phys.* 36 (1997) 1525.
- ⁴⁹ C. Hepburn, “Polyurethane Elastomers”, Applied Science Publishers, London (1982).
- ⁵⁰ H. Lu, Y. Obeng, K.A. Richardson, “Applicability of dynamic mechanical analysis for CMP polyurethane pad studies”, *Material Characterization* 49 (2002) 177.
- ⁵¹ H. Lu, B. Fookes, Y. Obeng, S. Machinski, K.A. Richardson, “Quantitative analysis of physical and chemical changes in CMP polyurethane pad surfaces”, *Material Characterization* 49 (2002) 35.
- ⁵² J.E. Ramsdell, “Characterization of chemical structure, morphology, and mechanical response of polyurethane surface domains as a result of exposure to common chemical mechanical planarization (CMP) environments”, Ph.D. Dissertation UCF (2001).

-
- ⁵³ S. R. Machinski, "Wear characterization of polyurethane chemical mechanical polishing pads", M.S. Thesis, UCF (2001).
- ⁵⁴ I. Li, "Chemical mechanical wear mechanism in polyurethane polishing pad materials", M.S. Thesis, UCF (2000).
- ⁵⁵ Y. S. Obeng, E. M. Yokley, U.S. Pat. 657 (2003) 9604.
- ⁵⁶ D. S. Rickerby, S. J. Bull, "Engineering with surface coatings: The role of coating microstructure", *Surf. Coat. Tech.* 39/40 (1989) 315.
- ⁵⁷ F. D. Egitto, L. J. Matienzo, "Plasma modification of polymer surfaces for adhesion improvement", *IBM J. Res. Develop.* 38 (1994) 423.
- ⁵⁸ Y. Z. Hu, G. R. Yang, T. P. Chow, R. J. Gutmann, "Chemical-mechanical polishing of PECVD silicon nitride", *Thin Solid Films* 290-291 (1996) 453.
- ⁵⁹ D. T. Price, R. J. Gutmann, and S. P. Murarka, "Damascene copper interconnects with polymer ILDs", *Thin Solid Films* 308/309 (1997) 523.
- ⁶⁰ D. R. Lide, and H. P. R. Frederikse, Editors, CRC Handbook of Chemistry and Physics, 78th edition, p. 8, CRC Press, Boca Raton (1997).
- ⁶¹ T. L. Barr, and S. Seal, "Nature of the use of adventitious carbon as a binding energy standard" *J. Vac. Sci. Tech. A* 13 (1995) 1239.
- ⁶² G. Beamson, and D. Briggs, High resolution XPS of Organic Polymers, Wiley, New York, (1992).
- ⁶³ T. L. Barr, "Modern ECSA", CRC Press, Boca Raton, Florida (1994).
- ⁶⁴ Evans East, www.evans-east.com
- ⁶⁵ W. C. Oliver, and G. M. Pharr, "Measurement of hardness and elastic modulus by instrumented indentation: Advances in understanding and refinements to methodology" *J. Mater. Res.* 7 (1992) 1564.
- ⁶⁶ W. C. Oliver, G. M. Pharr, "An Improved Technique for Determining Hardness and Elastic Modulus Using Load and Displacement Sensing Indentation Experiments" *Mater. Sci. Engg.* 7 (1992) 1564.
- ⁶⁷ A. C. Fischer-Cripps, "A review of analysis methods for sub-micron indentation testing" *Vacuum* 58 (2000) 569.

-
- ⁶⁸ S.Rajgopalan,R.Vaidyanathan, “Nano and Microscale Mechanical Characterization Using Instrumented Indentation”, *JOM* 54 (2002) 45.
- ⁶⁹ N. J. Mills and H.X. Zhu, “The high strain compression of closed-cell polymer foams” *J. Mech. Phys. Solids* 47 (1999) 669.
- ⁷⁰ M.Pourbaix, “Lectures on electrochemical corrosion”, Plenum press, London (1973).
- ⁷¹ C.W.Jones, “ Applications of Hydrogen Peroxide and Derivatives”, Royal Society of Chemistry, Cambridge (1999).
- ⁷² H. Hirabayashi, M. Higuchi, and K. Kabushiki, U. S. Pat. 557 (1996)5885.
- ⁷³ M. Hariharaputhiran, J. Zhang, S. Ramarajan, J. J. Keleher, Y. Li, and S. V. Babu, “Hydroxyl radical formation in H₂O₂-Amino acid mixture and chemical mechanical polishing of copper”, *J. Electrochem. Soc.* 147 (2000) 3820.
- ⁷⁴ L. Zhang, and S. Subramanian, “A model of abrasive-free removal of copper films using an aqueous hydrogen peroxide–glycine solution”, *Thin Solid Films* 397 (2001) 143.
- ⁷⁵ A. A. El-Shafei, M. N. H. Moussa, and A. A. El-Far, *J. Appl. Electrochemistry* 27 (1997) 1075.
- ⁷⁶ E. Szöcs, G. Vastag, and A. Shaban, “Investigation of copper corrosion inhibition by STM and EQCM techniques” *J. Appl. Electrochemistry* 29 (1999) 1339.
- ⁷⁷ W. Stephen Tait, “ An introduction to electrochemical corrosion testing for practicing engineers and scientists” , PairODocs Publication, Racine (1994).
- ⁷⁸ J. F. Moulder, W. F. Stickle, P. E. Sobol, and K. D. Bomben, in Handbook of X-Ray Photoelectron Spectroscopy, J. Chastian, Editor, Perkin-Elmer Corporation, Physical Electronics Division, Minnesota (1992).
- ⁷⁹ D. Chadwick, and T. Hashemi, “Adsorbed Corrosion Inhibitors Studied by Electron Spectroscopy--Benzotriazole on Cu and Cu Alloys”,*Corrosion Sci.* 18 (1978) 39.
- ⁸⁰ S. Aksu, and F. Doyle “Electrochemistry of copper in aqueous glycine solutions”, *J. Electrochem Soc.* 148 (2001) B51.
- ⁸¹ M.A. Karolewaski,R.G.Cavell, “ Characterization of adsorbed intermediates in the CH₃OH/O/Cu(100) system by secondary ion mass spectroscopy”, *Appl. Surf. Sci.* 173 (2001) 151.

-
- ⁸² K. Aramaki, T. Kiuchi, T. Sumiyoshi, and H. Nishihara, "Surface enhanced Raman scattering and impedance studies on the inhibition of copper corrosion in sulphate solutions by 5-substituted benzotriazoles" *Corros. Sci.* 32 (1991)593.
- ⁸³ N. Huynh, S.E. Bottle, T. Notoya, and D.P. Schweinsberg, "Inhibitive action of the octyl esters of 4- and 5-carboxybenzotriazole for copper corrosion in sulphate solutions", *Corros. Sci.* 42 (2000) 259.
- ⁸⁴ T. Notoya, T. M. Satake, T. Ohtsuka, H. Yashiro, M. Sato, T. Yamauchi and D. P. Schweinsberg, paper number 076 (<https://www.umist.ac.uk/corrosion/JCSE>), International symposium on "Corrosion Science in the 21st Century", July 6-11, 2003, UMIST, Manchester, UK.
- ⁸⁵ A.M.Mahajan, L.S. Patil, J.P.Bange, D.K.Gautam, "Growth of SiO₂ films by TEOS-PECVD system for microelectronics applications", *Surf. Coat Tech.* 183 (2004) 295.
- ⁸⁶ F. Tènégal, A. G. de la Rocque, G. Dufour, C. Sènémaud, B. Doucey, D. Bahloul-Hourlier, P. Goursat, M. Mayne, M. Cauchetier, "Structural determination of sintered Si₃N₄/SiC nanocomposite using the XPS differential charge effect" *J. Electron Spectro.* 109 (2000) 241.
- ⁸⁷ F. Fracassi, R. d'Agostino, P.Favia, "Plasma enhanced chemical vapor deposition of organosilicon thin films from tetraethoxysilane-oxygen feeds" *J. Electrochem. Soc.* 139 (1992) 2636.
- ⁸⁸ M.S. Hegde, R. Caracciolo, K.S. Hatton, J.B. Wachtman, "Electronic structure and bonding in silicon oxynitride films: An XPS study" *J. Appl. Surf. Sci.* 37 (1989) 16.
- ⁸⁹ W. J. Patrick, G. C. Schwartz, J. D. Chapple-Sokol, R. Carruthers, and K. Olsen, "Plasma-enhanced chemical vapor deposition of silicon oxide films using tetraethoxysilane and oxygen: characterization and properties of films", *J. Electrochem. Soc.* 139 (1992) 2604.
- ⁹⁰ M. G. J. Veprek-Heijman, and D. Boutard, "The hydrogen content and properties of SiO₂ films deposited from tetraethoxysilane at 27 MHz in various gas mixtures", *J. Electrochem. Soc.* 138 (1991) 2042.
- ⁹¹ S. Dakshinamurthy, "Instrumented nanoidetation studies of chemical mechanical polishing (CMP) pads", M.S. Thesis UCF (2003).